GLOBAL COMMISSION on the ECONOMICS OF WATER

TECHNICAL REPORT

The Impact of Water and Heat Stress from Global Warming on Agricultural Productivity and Food Security

Tom Kompas[1*], Tuong Nhu Che[2] and R. Quentin Grafton[3]

February 2023
watercommission.org

Author affiliations

[1]Centre of Excellence for Biosecurity Risk Analysis and Centre for Environmental and Economic Research, School of Biosciences and School of Ecosystem and Forest Sciences, University of Melbourne, Melbourne, Australia

[2]Australian Centre for Biosecurity and Environmental Economics, Crawford School of Public Policy, Australian National University, Canberra, Australia

[3]Crawford School of Public Policy, Australian National University, Canberra, Australia

*Corresponding author: Tom Kompas, Centre of Excellence for Biosecurity Risk Analysis and Centre for Environmental and Economic Research, School of Biosciences and School of Ecosystem and Forest Sciences, University of Melbourne, Melbourne, Australia 3010. Phone(s): +61 3 8344 3503, +61 418 600 144; email: tom.kompas@unimelb.edu.au.

Acknowledgements

Table of Contents

Acronyms

AEZ	agro-ecological zones
AEZ-EF	agro-ecological zone emissions factor model
CET	constant elasticity of transformation
CGE	computable general equilibrium
Gcal	Giga-calories
GIM	global irrigation model
Gm3	Giga cubic meters
GTAP	Global Trade Analysis Project
GWSWUSE	groundwater-surface water use model
IIASA	International Institute for Applied Systems Analysis
LSMs	land surface models ()
RCP	Representative Concentration Pathway ()
SDG	United Nations Sustainable Development Goals
SSP	shared socioeconomic pathways
WGHM	WaterGAP Global Hydrology Model

Executive summary

Global warming is a serious threat to agricultural production and food security. In this report, we present a unique large-dimensional computational global climate and trade model to simulate the impacts of irrigated water and heat stress on agricultural output, total food supply and food security to 2050, termed GTAP-DynW. The model uses GTAP data for 141 countries and regions, with varying water and heat stress baselines, and 65 commodity sectors, both aggregated into 30 countries/regions and 30 commodity sectors. The large dimension captures the heterogeneity of damages across the globe.

Along with a host of other data, the model also employs 18 AEZ land use categories and water use decompositions, with measures from WRI for irrigated water stress and heat stress indicators (as damage functions) from our previous work. The climate change scenarios examined are RCP4.5, RCP8.5-SPP2 and RCP8.5-SSP3. Model results indicate substantial falls (using a calorie metric) in the overall global food supply of 5.8%, 9.7% and 14.2% to 2050, with a resulting nutritional shortage or "food insecurity" for 556 million, 935 million and 1.36 billion additional people, compared to a 2020 baseline, for RCP4.5, RCP8.5-SSP2 and RCP8.5-SSP3, respectively.

Results are also indicated for individual commodities with paddy, wheat, cereal, livestock, meat (animal products) and dairy the most impacted, or with the largest losses in agricultural output.

Keywords: GTAP-DynW; climate change; water and heat stress; agricultural productivity; nutritional supply; food security.

JEL classification: C68, D58, Q25, Q54, O13.

1 Introduction

Water is essential for life, agricultural production, food security and economic activity. It is the lifeblood of global ecosystems, including forests, lakes, irrigated waterways and wetlands, on which our food and nutritional security depend (FAO, 2019). Global warming is a serious threat to water resources and the environment, both at the global and local levels (Bellie, 2011). Fecht (2019) points out that global warming is altering nearly every stage of the water cycle, such as groundwater flows, river discharge, stream flow, surface runoff, evaporation, precipitation, radiative exchange and water storage in ice and snow. These changes will put pressure on water supplies, agricultural production, socio-economic activities and the standard of living worldwide.

Overall, freshwater resources are dwindling, and the impact is intensifying due to increasing temperatures across the world (FAO, 2019). Although the exact impacts of climate change are hard to predict, there is a consensus that the global hydrological cycle will intensify and that extremes (e.g. floods, droughts) will occur more frequently and often with greater magnitude (Bellie, 2011). For agriculture, climate change and its impact on water resources pose one of the biggest challenges for agricultural and labour productivity, food supply and food security worldwide (Zolin and Rodrigues, 2020). Along with climate change, global economic development and population growth will also alter the availability of and competition for water worldwide (Luck et al., 2022).

Understanding ongoing climate change and its socio-economic impacts on current and future generations requires a comprehensive evaluation of the complex interplay between human and natural systems (see Roson and Sartori (2016) and Piontek et al. (2021)). The global economy, however, is complicated, with domestic and international input-output interactions crossing commodity sectors and regions, with variable endowments such as capital, labour, land, natural resources and water, along with essential productive inputs for each country, region and international trade. The agricultural sector, with substantial local production and international trade in food is especially complex. In such a case, computable general equilibrium (CGE) models provide a valuable tool for analysing potential damages from climate change as well as changes in policy instruments on the global economy. However, we need much more than a standard CGE model to capture the effect of changes in water resources and the impacts of climate change on agriculture and food security. We overcome this by constructing what we call GTAP-DynW, a unique intertemporal CGE model which further develops the GTAP-AEZ, Version 10 (Plevin et al., 2014) platform, with an extension for water uses from the GTAP-Water dataset (Iman et al., 2016). As such, GTAP-DynW provides the model context to incorporate dynamic changes in water resources and their availability on agricultural production, international trade and food security. The technical set-up builds on the modelling approach in Kompas and Van Ha (2019) and incorporates the added damages from global warming contained in Kompas et al. (2018) and Piontek et al. (2021).

In particular, GTAP-DynW is developed from GTAP-AEZ v10 with a number of distinctive features, including the decomposition of "sluggish" (non-moveable or slowly moving) land

endowments by 18 AEZs and, most importantly, water stress effects on AEZ land endowments and agricultural output. To simulate the impacts of water stress from global warming on agricultural production and food security to 2050, GTAP-DynW draws on the water stress indexes contained in WRI (2022a), covering three climate change and Shared Socioeconomic Pathways (SSPs) scenarios, or RCP4.5-SSP2, RCP8.5-SSP2 and RCP8.5- SSP3 for the decadal projections for the 2020s, 2030s and 2040s. Future agricultural outputs across a number of commodity sectors are projected from the model's calibrated results of time changes in output (in percentage terms) and the baseline output by sector and region (FAO, 2022a). Further, we analyse the consequences of future food security resulting from the reduction of agricultural output due to water and heat stress in two steps. First, we aggregate future food supplies as a sum of the nutritional supply from food commodities. Second, we estimate the number of people with "food insecurity" by dividing the reduction of food supply (as aggregated nutritional supply) by the average dietary requirements for a person per year. The aggregation of 141 countries in GTAP-DynW, with different baseline measures of water and heat stress, into 30 countries and regions, along with 30 commodity sectors, highlights the heterogeneity of damages across the globe.

Section 2 in this technical report provides the background to our study focus, including briefs on water consumption and irrigation, climate change impacts on water stress, heat stress effects, and the basics of global food security. Section 3 provides a literature review of the relevant modelling approaches, focusing on water stress impacts on agricultural production and the effects of climate change. Sections 4 and 5 present our methods and GTAP-DynW model structure. Section 6 details data sources, projections of water stress by WRI (2022a) and key assumptions. Section 7 reports modelling results for the projection of agricultural production, losses in productivity and food supply and food insecurity by climate change scenario. Section 8 offers some closing remarks.

2 Background

This section provides the context supporting our technical report, including briefs on: (a) global water consumption and irrigation, (b) climate change impacts on water stress, (c) heat stress effects on agricultural yield and labour productivity, and (d) implications for food security resulting from the decline in food supply due to water stress.

2.1 Water consumption and irrigation

Water resources primarily contain the sources from rain-fed water (green water) and water withdrawals (blue water). While green water is the evapotranspiration of precipitation, blue water refers to total water withdrawals for agriculture, industry and municipal or domestic uses (not counting evaporation losses from storage basins). Water from desalination plants, essential in some regions, is also included (Ritchie and Roser, 2022). From 1961 to 1990, on average, rain-fed water was 5,300 Giga cubic meters (Gm^3) and water withdrawals were 4,300 Gm^3 per year. The primary uses of blue water are for agricultural irrigation (73.6%), households (7.6%), electricity generation (12.2%), manufacturing (6%) and livestock (0.6%) (Müller Schmied et al., 2021).

Despite the growth rates of global freshwater slowing since 2000 (after increasing sharply from the 1950s onwards), freshwater use has multiplied. Driven significantly by worldwide population and economic growth, freshwater withdrawals have increased more than eight-fold from 500 Gm^3 in 1900 to more than 4,000 Gm^3 at present (Ritchie and Roser, 2022; Müller Schmied et al., 2021). While freshwater use has grown worldwide, the share of consumption among country groups has been relatively stable over the last century. In particular, OECD nations use approximately 20–25% of this water; BRICS countries (Brazil, Russia, India, China, and South Africa) account for the most significant share at approximately 45%; and ROW (Argentina, Australia, Brazil, Canada, India, Mexico, Russia, South Africa, Switzerland and Türkiye) at 30–33% (Ritchie and Roser, 2022).

Since the beginning of cultivation, irrigation water has reduced farmer dependence on rainfall, increased crop yields and boosted overall crop production (Fischer et al., 2007). Currently, irrigated areas have expanded to over 311 million hectares worldwide, almost 20% of total cultivated land (Iman et al., 2016). Being the most significant water user among human activities with about 2,982 Gm^3 per year (Iman et al., 2016), agriculture and food supply are most vulnerable to any water stress resulting from climate change (Müller Schmied et al., 2021).

The role of irrigation varies by country depending on geographical conditions, rain-fed water patterns and the demand for industry and municipal use. For example, in England, where rain is (currently) relatively abundant year round, irrigation accounts for a small fraction of human usage. However, irrigation exceeds 70% of total use in Spain, Portugal and Greece. Irrigation is also essential in many developing countries, which have faced food security challenges for centuries, with irrigation accounting for over 90% of water withdraws (WBCSD, 2005). The average agricultural water use for low-income countries is 90%, 79% for middle income, and only 41% for high income countries (Ritchie and Roser, 2022). Regarding concerns over end-use water consumption, irrigation efficiency is an important consideration. Roughly 5–35% of irrigation withdrawals are unsustainable due to leaking and evaporating from irrigation canals and pipes, and an estimated 15–35% of irrigation withdrawals are unsustainable (WBCSD, 2005).

Water for industrial uses includes dilution, steam generation, washing, cooling of manufacturing equipment, thermal power plants, use in nuclear power plants and wastewater from industrial processes (Ritchie and Roser, 2022). Worldwide, the United States is the largest industrial water user, withdrawing over 300 Gm^3 per year. The second largest is China, which is far less at 140 Gm^3 per year (Ritchie and Roser, 2022). Water for industrial uses is more than 1 Gm^3 in most countries across the Americas, Europe, East Asia and the Pacific regions. Across sub-Saharan Africa and some parts of South Asia, industrial water is much lower at less than 0.5 Gm^3.

Municipal water is for domestic or household purposes, or public services (Richie and Roser, 2022). Municipal waters are for drinking, cleaning, washing and cooking. Driven by the world's largest population, China's domestic water demands are over 70 Gm^3 per year. The second most populous country, India, is the third largest municipal water user. The United States is the second largest user due to higher per capita water demands. The share of municipal water over total usage in some countries across sub-Saharan Africa is relatively high due to low requirements for agricultural and industrial withdrawals (Ritchie and Roser, 2022).

2.2 Climate change impacts on water stress

Water stress is defined as the ratio of water demand for social-economic activities divided by available water (Taylor et al., 2012). It is also commonly known as the withdrawals-to-availability ratio or relative water demand (Gassert et al., 2014). According to Dolan et al. (2021), water stress is dynamic and complex, influenced by climate change, basin-level water resources and water systems adaptation. According to World Bank (2016), the impacts of climate change would primarily affect the water cycle, with consequences that could be large and uneven, generating risks to the food supply, energy production and the environment. With population, economic growth and urbanisation, the global demand for water rises expo-nentially, while water supply becomes more unstable and uncertain (Dolan et al., 2021). Along with the climate change process, the threat of water stress and scarcity is a critical challenge for agriculture and food security.

In agriculture, water resources which depend on irrigation and rain-fed water, are a crucial driver and key input (Fischer et al., 2007). By 2050, a scenario analysis shows that 59% of the world population will face a blue water shortage, and 36% will face green and blue water shortages (Rockström et al., 2009). WRI (2022a) also projects that global warming will increase the number of water-stressed areas and heighten water stress. The increase in water stress could also deteriorate the number of freshwater resources (aquifer over-exploitation, dry rivers, etc.) and their quality (organic matter pollution, saline intrusion, etc.) (EEA, 2022).

2.3 Heat stress effects

Following (Kompas et al., 2018), this technical report also includes the impact of heat stress on agricultural yields and labour productivity, which extends the climate change damage functions and relevant parameters in Roson and Sartori (2016). Damage functions provide the relationships between climate variables (such as average temperature, humidity, or heating days) and productivity, income, resource endowments, and so on (Roson and Sartori, 2016). Roson and Sartori (2016) present the methodology and estimated parameters of damage functions for 120 Global Trade Analysis Project (GTAP) countries and regions using GTAP9 with six climate impacts: sea level rise, variation in crop yields, heat effects on labour productivity, human health, tourism and household energy demand. In our technical report, we focus only on heat stress in terms of losses in agricultural and labour productivity, and we use the current version of GTAP data, GTAP10a.

2.4 Global food security

Irrigation is critical for agricultural production, ensuring food security for human life across the globe. As the world economy has developed, nevertheless, so has the gap in living stand-ards and inequality. At present, roughly 850 million people worldwide are currently under-nourished (FAO, 2020d), more than 2 billion individuals experience critical micro-nutrient defi-ciencies, and as many as 60% of individuals in some low-income countries are food insecure (Pérez-Escamilla, 2017). Although the United Nations Sustainable Development Goals (SDGs) are defined to ensure food security (Pérez-Escamilla, 2017), a state where people have access to sufficient nutrition to meet dietary needs for a healthy and active life, the commitment made in 2015 to reducing hunger by half (World Food Summit and Millennium Development Goals) has resulted in little change since the 1990–92 base period (FAO, 2020d). In this report,

we simulate the further increase in the number of individuals as a percentage of the population that are food insecure, or do not meet minimum daily calorie intake (i.e. a basic abundance measure), by country, relative to a given 2020 baseline.

3 A brief literature review

This section briefly reviews a number of publications relevant to the impacts of water stress on agricultural production by climate change scenario.

To begin, Zolin and Rodrigues (2020) provide a multi-disciplinary approach to climate change and water resource availability, highlighting the hydrological cycle, forests, land-use change, water and agriculture. This is useful, but several publications go a step further with specific modelling and applications.

Regarding the impacts of irrigation water on agricultural yield, for example, Grafton et al. (2017) employs a "bottom-up" field-based, crop-hydrological model for estimating food production and irrigated water extractions under multiple scenarios of water and nitrogen use, along with crop yield increases from 2010 to 2050 for 19 countries.

Zhao et al. (2020) estimates the effects of different levels of water stress on photosynthesis, growth, yield, water use efficiency (WUE) and irrigation water productivity (IWP) for winter wheat. According to Zhao et al. (2020), scenarios for mild, moderate and severe water stress levels would reduce wheat yield by 7.4%, 29.6% and 44.4%, respectively.

Sadras et al. (2017) establishes that the relative reduction in agricultural yield is directly proportional to the relative decrease in water supply. The empirical coefficient of water stress on crop yield here ranges from 0.8–1.5. However, this coefficient is assumed to increase considerably over time, with projected water stress coefficients ranging from 0.5–0.6 (Low Case), 0.9–1.1 (Medium Case) and 1.2–1.5 (High Case).

Based on a combination of global, crop-specific, hydrological modelling and experimental observations, Dolan et al. (2017) analyses non-renewable groundwater abstraction and food trade data to estimate the rates of groundwater depletion embedded in international food trade. The study shows that approximately 11% of non-renewable groundwater for irrigation is embedded in food trade, with food exports from Pakistan, the USA and India accounting for two-thirds of the total. According to Dolan et al. (2017), the risks to international food trade and water security are highlighted because a significant part of the world population is located in countries that depend on major staple crop imports from exporters who deplete groundwater to produce these crops. In particular, some countries, like the United States, Mexico, Iran and China, are at high risk due to both producing and importing food irrigated from rapidly depleting aquifers.

WaterGAP is a global hydrological model of water resources which estimates the consumption of groundwater and surface water, along with water flows and storage (Müller Schmied et al., 2021). The model (developed in 1996) assesses both water resource availability and water stress. Based on Müller Schmied et al. (2021), WaterGAP 2.2 contains three major

components: a global water use model, a linking Groundwater-Surface Water Use Model (GWSWUSE) and the WaterGAP Global Hydrology Model (WGHM). Five global water models for irrigation, livestock, households, manufacturing and the cooling of thermal power plants, are employed for estimating consumptive water and water withdrawals. While the Global Irrigation Model (GIM) for irrigation is monthly, all non-irrigation water use models are in annual time series. The linking model GWSWUSE, which distinguishes water use from groundwater and surface water bodies, estimates withdrawal water uses from and return flows to the two alternative water sources, to generate a monthly time series of net abstractions from surface water and groundwater. Given our purposes in this study, WaterGAP 2.2 is not very useful because it only focuses on five sectors of water users, which limits analysing water impacts on the global economy, where (most importantly for our purposes) demand and supply are balanced for all goods and services and endowments, with international trade. In addition, the application of the model in Müller Schmied et al. (2021) has yet to provide a long-term outlook of water supplies under the effect of different climate change scenarios.

GCAM v5.1, on the other hand, is a global-to-basin-scale model of potential water stress impacts, which has been applied to a number of publications, such as Dolan et al. (2021) and World Bank (2016). According to Calvin et al. (2019), GCAM v5.1 is a recursive model with technology factors for the energy sector, land use and water linked to a climate model for implementing various climate policies. This global model represents the behaviour and interactions between five systems: the energy system, water, agriculture, land use, the economy and the climate (Calvin et al., 2019). The model is in five-year time steps with 22 step runs for the period of 1990–2100 and a decomposition of the world into 32 geopolitical regions, 384 land-use regions and 235 water basins. GCAM includes coupled representations of the earth's climate, economic, hydrological, land-use and energy systems. Population and GDP growth are exogenous model inputs. Energy and land-use systems are modelled in more detail, with shares of supplies and technologies competing using a statistical model. Under the assumptions of population and labour productivity growth, and the energy and land-use systems (with numerous technology options), the model explores changes in energy supplies, agriculture and forest products that lead to land use and land cover changes. GCAM also has been used to explore the potential role of emerging energy supply technologies and the emission consequences with various Representative Concentration Pathway (RCP) scenarios. Further details of the model are provided by Calvin et al. (2019).

By linking the GCAM v5.1 model, Dolan et al. (2021) develops a global hydrological model and the loss of economic surplus driven by resource shortages. Dolan et al. (2021) shows that major hydrological basins can experience intensely positive or negative economic effects due to the dynamics of global trade and market adaptations to resource shortages. In many cases, market dynamics could cause significant economic uncertainty relative to hydrological uncertainty. The negative economic impacts due to international trade dynamics in Dolan et al. (2021) also suggest a need to represent the interactions of global trade markets, albeit with only five sectors included in GCAM.

Given our purposes in this study, GCAM has limitations compared to GTAP-DynW. First, GCAM v5.1 covers water supply and demand by region for energy and agriculture, assuming (within context) that water supply is an unlimited resource. This makes it difficult to project the comprehensive impacts of water stress (the withdrawals-to-supply ratio) under various climate change scenarios. Second, the model covers only five sectors without sufficient inter-

national trade flows. This is the key benefit of GTAP modelling, with full interactions and trade flows for exports and imports for up to and across 141 countries. Unlike GTAP-DynW, GCAM also does not represent the global (and local) market clearing for produced goods and factor endowments such as capital, labour and natural resources (including water). The effects of water stress on global and regional economic activities, trade, demand and supply, need to be sufficiently explored in the more general setting that GTAP-DynW represents. Finally, land use in GCAM only consists of energy and agriculture, which excludes consideration for land use in many other economic sectors (e.g. services, transport, industries, forests, etc.), and with a 22-step run at a five-year interval, the model results do not provide a dynamic annual path for key variables. Simulations to 2050 would thus be especially limited.

4 Methods

Our GTAP-DynW model is a large dimensional computable general equilibrium (CGE) model, primarily based on an extensive GTAP (Global Trade Analysis Project) data set Version 10a. GTAP is an essential tool for researchers and policymakers conducting quantitative analysis of changes in produced output, trade patterns and commodity flows (Hertel, 1997; GTAP, 2021). In its current form, a GTAP model (and its accompanying database) is a trade model where countries or regions interact, importing goods and services from each other. In each country, a producer combines inputs (land, labour, capital, intermediate good and natural resources) to produce a single good or service, which is consumed domestically by regional households (i.e. final consumption) and producers (i.e. intermediate demand for products as inputs in the production of other commodities), or is exported to other international or regional households and producers. Producers maximise current profits given inputs and output prices, and households earn income from selling productive inputs and then allocate this income to consumption expenditures and savings. A government sector is also included, with associated expenditures and tax revenues.

The GTAP framework we employ is a unique computational approach using an intertemporal optimisation routine. Following Kompas and Van Ha (2019) and Kompas et al. (2018), for climate change damage functions, the standard CGE producer problem is accordingly extended to a forward-looking problem, where the producer can maximise profits over the long run taking into account future impacts and policy settings. In particular, the component solution for the forward-looking producer problem that is different from the traditional recursive GTAP model can be summarised in terms of a system of motion equations:

$$\dot{k}_{r,t} = \psi_{r,t} - \delta_r k_{r,t} \tag{1}$$

$$\dot{\mu}_{r,t} = \mu_{r,t}[i_t + \delta_r] - \frac{\phi_r}{2}\left(\frac{\psi_r}{k_{r,t}}\right)^2 p_{r,t}^I - p_{r,t}^K \tag{2}$$

where $p_{r,t}^K$ and $k_{r,t}$ are the rental price of capital and the capital stock in region r at time t; $p_{r,t}^I$ is the price of an investment good; δ_r is the depreciation rate; ψ_r is the capital increment from the (gross) investment activity; i_t is the global interest rate; φ_r is an investment increment coefficient; and $\mu_{r,t}$ is the shadow price of capital.

While the capital accumulation process in a forward-looking model (equation 1) is similar to that of a standard recursive GTAP model, the shadow price of capital equation (equation 2) allows for a connection between future price dynamics to the producer's current period decision-making process. This offers three key advantages. First, the framework can be placed in a large dimensional setting incorporating a large number of produced commodities and countries or regions. This allows model output to capture the full heterogeneity of damages from global warming across countries (see Piontek et al. 2021). Averaging across countries, or using small dimensional platforms, misses the full distribution of damages and severely distorts the results. Second, forward-looking firms (or households) can incorporate future changes into current planning (e.g. emissions reduction targets, a price on carbon, price and output changes from global warming, etc.), rather than "forecasting" next year's prices/outputs based only on current and past values. This matters greatly for climate change modelling. Finally, the model can be fully integrated with established RCPs and SSPs, connecting global warming to changes in country output and international trade.

GTAP-DynW extends this intertemporal approach to AEZ land use decomposition, irrigation water use by AEZ, and the impacts of global warming from water and heat stress on agricultural productivity and output. Specifically, we use land characteristics as a combination of soil, land-form and climatic features as applied by the Food and Agricultural Organization FAO (2022b) to classify global land use by 18 agro-ecological zones (AEZ). According to Ahmed et al. (2016b), GTAP-AEZ differs from the standard GTAP approach by including additional elements for analysing land use and emissions. As such, GTAP-AEZ allows land endowment to be heterogeneous, and thereby the regional land endowment is split into agro-ecological zones by climatic zones and land characteristics. Due to regional land being a "sluggish" (i.e. non-moveable or slowly moveable) endowment, GTAP-AEZ applies limited land mobility to follow a constant elasticity of transformation (CET) function. A further study by Plevin et al. (2014) develops the agro-ecological zone emissions factor model (AEZ-EF) for estimating the total emissions (carbon equivalent) from land use changes.

A study by Iman et al. (2016), which we employ, introduced water into a GTAP database by dividing the crop sectors of the GTAP power database into irrigated and rain-fed categories. By river basin at the AEZ level, Iman et al. (2016) included irrigated water into the cost structure of irrigated crops. Currently, the database, which is in progress, has more than 700 variables of AEZ types, which are different land features for 19 regions. In GTAP-DynW, the GTAP-AEZ, Version 10 is linked to the GTAP-Water dataset by AEZ and region by Iman et al. (2016). We merge AEZ land use by water content in terms of irrigation circulation per year by crop and the share of irrigated area in the total land (see a summary in Table 1). Given that the water element is incorporated into AEZ land use, a defined shock from water stress changes the effectiveness of land use endowments and thus impacts agricultural productivity and output for a variety of commodities.

5 Model structure

GTAP-DynW is developed from the GTAP structure and Kompas and Van Ha (2019) using GTAP-AEZ v10 with distinctive features, including the decomposition of sluggish land endowments by 18 AEZs and water stress impacts on AEZ land endowments and agricultural productivity. As indicated, by linking to the dataset of GTAP-Water by Iman et al. (2016) for irrigated water use by AEZ categories, regions and agricultural land and sectors, GTAP- DynW provides a key tool for simulating the impacts of water stress on land use and farming outputs. The model also captures a heat stress effect from global warming and estimates the losses in food supply and food security, as well as the percentage of the population (by country) under threat of food insecurity due to climate change impacts. Here, we outline the model structure in detail.

5.1 Decomposition of land endowments

We follow Lee (2004), who acknowledges that the FAO and IIASA (International Institute for Applied Systems Analysis) have developed an agro-ecological zoning methodology that segments land into smaller parcels according to agro-ecological characteristics (e.g. moisture and temperature regimes, soil type, land-form, etc.). Each AEZ has similar constraints, characteristics and potential land use. The FAO/IIASA agro-ecological zoning methodology provides a standardised framework for characterising climate, soil and terrain conditions pertinent to agricultural production.

Along with the GTAP model structure, GTAP-DynW follows a "top-down" GTAP approach for GTAP-AEZ Version 10a.[1] The GTAP-AEZ database and theoretical structure differ from the standard GTAP model. They include additional elements to allow an analysis of land use and emissions by AEZs (Ahmed et al., 2016b). In particular, as indicated previously, GTAP-AEZ provides a heterogeneous endowment land use with regional land endowment decomposed into 18 AEZs, which can differ by growing period and climatic characteristics. The GTAP-AEZ database also recognises that land may be unrestricted between alternative uses. Land mobility itself is characterised by a constant elasticity of transformation (CET) frontier with different returns to land in alternative uses (Ahmed et al., 2016a). Also, following Ahmed et al. (2016a), the GTAP-AEZ database allows for changes in crop yields by extensive and intensive margins, and for emissions targeted from land use changes. The precise mapping of AEZs to regions in GTAP-DynW is indicated in Table 1.

---

[1]The "bottom-up" (engineering) approach, on the other hand, often starts with detailed energy-producing processes or technology bundles and then explores the question that, given a particular level of demand for energy to produce various outputs, what is the most efficient, cost-minimising way of meeting these demands in terms of the energy technologies employed and the level and mix of inputs needed to produce energy (Covey and Truong, 2002).

Table 1. Baseline irrigated water circulation by AEZ and region in GTAP-DynW (Mil m³/year)

Region	AEZ1-18																	
	aez1	aez2	aez3	aez4	aez5	aez6	aez7	aez8	aez9	aez10	aez11	aez12	aez13	aez14	aez15	aez16	aez17	aez18
aus	10	37	756	66	0	0	1,354	686	1,130	434	703	131	-	-	0	1	-	-
bra	-	167	87	554	622	156	-	-	-	0	3	1,214	-	-	-	-	-	-
caf	5,215	890	571	319	111	1,539	645	18	161	214	150	212	-	-	-	-	-	-
cam	-	-	69	727	843	325	-	-	-	84	23	2	-	-	-	-	-	-
can	-	-	-	-	-	-	-	37	2	5	17	-	114	23	2	0	-	-
ceu	-	-	-	-	-	-	-	-	-	710	-	-	-	0	0	0	-	-
chn	-	-	-	114	498	492	133,712	62,946	112,653	19,649	17,909	48,444	1,735	90	281	0	-	-
deu	-	-	-	-	-	-	-	-	150	206	114	-	-	-	0	-	-	-
eao	-	-	-	-	-	-	0	4	157	1,759	1,134	-	1	7	111	-	-	-
eew	-	-	-	-	-	-	37,059	52,015	2,364	695	16	2	27	1,399	7	0	-	-
fra	-	-	-	-	-	-	-	38	40	197	569	34	0	0	0	0	-	-
gbr	-	-	-	-	-	-	-	-	-	89	258	8	-	-	0	0	-	-
ind	65	16,318	86,363	44,477	707	-	19,065	86,927	107,941	9,321	974	1,177	-	-	-	-	-	-
ita	-	-	-	-	-	-	-	46	29	95	421	4	0	0	0	-	-	-
jpn	-	-	-	-	-	-	-	-	173	6,743	16,794	9,084	-	-	173	-	-	-

Region — AEZ1-18

Region	AEZ1	AEZ2	AEZ3	AEZ4	AEZ5	AEZ6	AEZ7	AEZ8	AEZ9	AEZ10	AEZ11	AEZ12	AEZ13	AEZ14	AEZ15	AEZ16	AEZ17	AEZ18
kor	-	-	-	-	-	-	-	-	-	532	836	-	-	-	-	-	-	-
mex	10,690	2,859	5,535	1,219	390	84	8,301	3,557	7,093	1,087	58	2	-	-	-	-	-	-
naf	588	102	53	17	2	265	4,544	83	270	380	148	901	-	-	-	-	-	-
nsa	6,225	878	2,165	2,158	3,415	1,045	2,344	1,674	396	409	44	194	-	-	-	-	-	-
nzl	-	-	-	-	-	-	-	0	25	69	248	623	-	-	0	12	-	-
osa	585	232	246	95	7	198	470	41	131	77	61	49	-	-	-	-	-	-
rus	-	-	-	-	-	-	-	511	165	73	0	-	27	28	33	-	-	-
sas	24,604	-	263	6,095	7,466	1,142	398,747	24,088	20,619	22,363	1,397	3,864	1	-	-	-	-	-
ssa	-	-	156	63	35	12	9,996	5,139	1,240	1,892	121	406	90	740	193	31	0	-
tur	-	-	-	-	-	-	67	7,938	1,871	158	8	0	0	24	2	-	-	-
usa	-	-	-	-	-	-	21,692	21,550	7,898	1,077	1,064	1,916	189	185	2	0	-	-
weu	-	-	-	-	-	-	-	72	655	263	332	25	0	5	1	0	-	-
zaf	44	18	5	0	0	-	539	148	208	122	41	4	-	-	-	-	-	-
asean	-	-	24,762	26,678	58,641	-	-	-	-	0	19	190	-	-	-	-	-	-
me	331,627	-	-	-	-	-	332,770	60,985	10,242	1,255	-	-	-	-	-	-	-	-
Sum by AEZ	379,652	21,502	96,270	80,667	40,775	63,898	971,306	328,502	275,613	69,957	43,461	68,488	2,184	2,502	804	45	0	-

Note: Authors' calculation of baseline irrigated water based on Iman et al. (2016) and Chepeliev (2020). See Table A1 in Appendix A for relevant country and region codes.

5.2 Water stress and land endowments

To account for water stress, GTAP-DynW links GTAP-AEZ with 18 AEZ sluggish land endowments with the water use features computed from the GTAP-Water data by AEZ, by region and agricultural sectors (Iman et al., 2016). In particular, the AEZ land endowments are incorporated into baseline irrigated water by AEZ, by region, and farming sectors computed from the GTAP-Water database by (Iman et al., 2016). The data from Iman et al. (2016) and Ahmed et al. (2016b) are estimated for 30 regions aggregated for GTAP-DynW. Table 1 again summarises the irrigated water circulation per year by AEZ and the GTAP-DynW regions.

The production of agriculture output ($Qo_{j,t}$) is structured as a constant elasticity substitution (*CES*) production function, including the demand for commodity *i* for use by *j* ($QF_{i,j,t}$) from both domestic and imported sources, and the value added in the industry *j* ($QVA_{j,t}$). The demand of sluggish endowments ($QSE_{i,j,t}$) (which contains 19 endowment commodities, including 18 AEZ land use categories and natural resources) for the value added in the industry *j* ($QVA_{j,t}$) is given by

$$QSE_{i,j,t} = \left[\frac{QVA_{j,t}}{afe_{i,j,t}}\right]\left(afe_{i,j,t}\frac{PVA_{j,t}}{PSE_{i,j,t}}\right)^{\gamma_{j,t}} \tag{3}$$

where $afe_{i,j,t}$ is augmenting technological change of the sluggish endowments *i* by *j*; $PSE_{i,j,t}$ is the market price of sluggish endowment *i* used by industry *j*; $PVA_{j,t}$ is the firm's price of value added in industry *j*; and $\gamma_{j,t}$ is the elasticity of transformation for sluggish primary factor endowments in the production of value-added in *j*.

Under the effect of water stress (the deviation from the baseline resulting from climate change), the effectiveness of land use for agriculture or AEZ land zones decreases, where the relative reduction in the efficiency of land endowments is directly proportional to the relative increase in water stress. It follows that shocks to land use by AEZ by region and time in $QFE_{i,j,t}$ will change $QVA_{j,t}$ and as a result agricultural production $Qo_{j,t}$.

The shock of AEZ land use by region in equation (3) is derived from the deviation of water stress from the baseline over time under the effect of climate change following WRI (2022a). Note that the water stress can be the result of too much or too little water.

With WRI (2022a), the effect of water irrigation in AEZ land use on agriculture is assumed to impact irrigated land only. AEZ land use is decomposed into irrigated (blue water) and rain-fed harvested area (green water) by Iman et al. (2016), thereby the shock of AEZ land use depends on the share of irrigated land in total land use in the region's AEZ ($w_{c,irr}$) and the change of irrigated water volume in that AEZ in a region ($dIW_{c,t}$), given by

$$QSE_{i,j,t} = \frac{\widehat{L(c,irr)}}{L(c)}dIW_{c,t} \tag{4}$$

where *c, j, t* represents 18 AEZ land types, agricultural commodity and time.

5.3 Water stress and agricultural output

To calibrate the impact of water stress on agricultural output, we introduce a constant elasticity of substitution (*CES*) production function and define industry demands for intermediate inputs ($QF_{i,j,t}$) by

$$QF_{i,j,t} = \left[A_{i,j,t} \frac{Q_{j,t}}{afw2_{j,t}\left(\frac{pf_{e,j,t}}{afw1_{i,t}} \frac{1}{ps_{j,t}}\right)^{\gamma_{j,t}}} \right] \tag{5}$$

where $Q_{j,t}$ is the agricultural output of commodity j; $pf_{i,j,t}$ is the firm's price for input commodity i for use by j; $ps_{j,t}$ is the supply price of commodity j; $A_{i,j,t}$ is the composite regional variable of augmenting technology change; and $\gamma_{j,t}$ is the elasticity of substitution among composite intermediate inputs in the agricultural sector j.

In equation (5), $A_{i,j,t}$ is a regional composite variable of augmenting technological change of intermediate input i for j, including the intermediate input augmenting technological change factor ($afall_{i,j,t}$). For our purposes, GTAP-DynW adds two specific augmenting technology change variables. They are the augmenting water stress factor ($afw1_{i,t}$) for intermediate inputs and endowments used for production, and the region-specific average rate of intermediates augmenting technology change of j ($afw2_{j,t}$). In equation (5), an increase in $afw1_{i,t}$ reduces the effectiveness of inputs and endowments required for producing a unit of agricultural output, resulting in lower $Q_{j,t}$.

Given the effect of irrigated water stress on irrigated areas and selected crops, the shock of $afw1_{c,j,t}$ depends on the weighted coefficient of irrigated land in total land use for an agricultural crop $w_{irr,j}$, the change of irrigated water by time ($dIW_{c,t}$), and the water stress coefficient to crop yields, or

$$dafw1_{c,j,t} = \overbrace{\frac{L(c,j,irr)}{L(c,j)}}^{w_{irr,j}} \frac{1}{dIW_{c,t}} ws_{c,j,t} \tag{6}$$

where c, j, t presents 18 AEZ land types, agricultural commodity and time. In equation (6), the shock $dafw1_{c,j,t}$ will increase with a larger share of irrigated area and a higher water stress coefficient.

5.4 Water prices for user industries

GTAP-DynW also incorporates a water price analysis to GTAP-AEZ that allows us to investigate the case of water prices imposed and their impacts on shifting water resources among industries. Water prices from water resources paid by water user industries are added to regional income, but also increase costs in these sectors that may cause a shift or reallocation of water use among water user industries.

With water price *pwater*(t) in a region *r*, the price index for purchases of *k* commodity by *j* sector in region *r* ($PFE_{j,k,r,t}$) is given by

$$PFE_{j,k,r,t} = \left[p_{j,k,r,t} + taxF_{j,k,t} \right] + \left(\frac{pwater_{r,t} WIN_{j,k,r,t}}{VFA_{j,k,r,t}} \right) \tag{7}$$

$VFA_{j,k,r,t}$ is the purchases and firm's tax of *k* inputs for use by sector *j*; $p_{j,k,r,t}$ is the market price of *k* to *j*; $taxF_{j,k,r,t}$ is the tax on firm's purchases of *k* by production *j*; $pwater_{r,t}$ is water price at *t*; and $WIN_{j,k,r,t}$ is the water intensity of *j* on *k*.

The shock on water prices $pwater_{r,t}$ will cause $PFE_{j,k,r,t}$ to change, causing the demand of *j* to fall and water resources will be shifted to other water users. The shock of water prices can be applied to both domestic and imported water sources.

5.5 Heat stress effects

In equation (5), $A_{i,j,t}$ is a regional composite variable of augmenting technology change of intermediate input *i* for *j*, including $afall_{i,j,t}$. The heat stress shocks from global warming (e.g. losses in agricultural and labour productivity), based on Kompas et al. (2018), Kompas and Van Ha (2019), and Roson and Sartori (2016), are applied to $afall_{i,j,t}$ in GTAP-DynW.

5.6 Nutrition (calorie) supply and food security

Each food commodity contains nutritional components with different energy intake (calories). The aggregated nutritional supply in the region *r* (*S*(*r*, *t*)) (measured as Giga-calories (Gcal)) is aggregated as a sum of nutritional supply from food supply *i* or

$$S(r,t) = \sum_{i=1}^{I} \frac{S(i,r,t)z(i)*1000}{10^9} \tag{8}$$

where *S*(*i*, *r*, *t*) is the supply of food *i* (thousand tons); and *z*(*i*) is the nutrition conversion factors of food *i* for calculating that food's energy content from one ton of food *i* to calories. The average daily nutrition intake *a* required for human food security is taken as given, and varies by country and region (FAO, 2020a, 2020b, 2020c). Translating to total population (*F* (*r*, *t*)) gives

$$F(r,t) = \frac{S(r,t)*10^9}{a*365*10^6} \tag{9}$$

where *a* is average daily nutrition in calories. The global food supply (Gcal) is the sum of all regional food supply and the total population across regions is *F* (*t*).

Under the effects of water and heat stress, the food supply at time t will decrease (computed from the model's calibrated results and the baseline quantity supplied (in tonnes)). The number of "food insecurity" persons (millions) resulting from the decrease in food supply in r, using a basic abundance measure, or $IF(r, t)$, is measured by

$$IF_{r,t} = \frac{\overbrace{[S(r,0) - S(r,t)]}^{dS_{r,t}} 10^9}{a * 365 * 10^6} \quad (10)$$

where $dS(r, t)$ is the reduction of food supply in region r at t to the base nutritional supply ($S(r, 0)$).

The food insecurity rate ($RIF(r, t)$) as the percentage of the number of persons with severe food shortage over the total population of that country or $POP(r, t)$ is

$$RIF(r, t) = \frac{IF(r,t)}{POP(r,t)} \quad (11)$$

The global reduction of food supply ($dS(t)$) is the sum of the reduction of food supply ($dS(r, t)$) across all regions. The global number of persons with food insecurity ($IF(t)$) is the sum of all regions' food insecure persons resulting from the reduction of food supply (or $IF(r, t)$).

6 Data sources and key limitations

6.1 Data sources

The GTAP data for GTAP-DynW is the GTAP-AEZ database Version 10a (GTAP, 2021), which is calibrated for the world economy across 65 (tradeable) commodity sectors for 141 countries/regions (with the base year 2014). These 141 countries/regions account for 98% of world GDP and 92% of the world's population (Aguiar et al., 2019). In GTAP-DynW, the countries/regions and commodity sectors are aggregated into 30 countries/regions and 30 sectors (see Appendix A and B for details). The GTAP-DynW sluggish land endowment is disaggregated into 18 categories by (Aguiar et al., 2019). It is important to note that countries listed within a given region have different water and heat stress baselines.

The supporting database of agricultural production and land in each GTAP-DynW region is drawn from FAO (2022a). Thirteen agricultural sectors are analysed, including: paddy; wheat; cereal; vegetables[2]; oilseed; sugar can; fibres; other crops; livestock; poultry; meat and animal products; dairy and wool.[3]

We incorporate GTAP-DynW's data for AEZ regions and industries with the irrigation water data from GTAP-Water data (Version 9) (GTAP, 2021) as analysed by Iman et al. (2016). GTAP-DynW's database represents cropping activities in eight distinct sectors: paddy rice, wheat, coarse grains, vegetable and fruits, oilseed, sugar crops, plant-based fibre and other crops. AEZ land use is decomposed into irrigated and rain-fed harvested area from Iman et al. (2016) for these eight distinct sectors. Overall, irrigated yield is higher than rain-fed yield (Iman et al., 2016). The share of irrigated area in total cropland by AEZ, region and agricultural industries is based on Iman et al. (2016). GTAP-DynW's 30 regions concord with aggregated areas from Iman et al. (2016).

Geographical data sources for global aqueduct water by basins and countries are drawn from WRI (2022b) and analysed in Gassert et al. (2014). Projections of water stress by climate change scenario are from WRI (2022a) and Luck et al. (2022). Other global Geographic Information System (GIS) spatial data are from Esri-USGS (2022).

We also apply the parameter of water stress impacts on wheat for RCP4.5 and RCP8.5 from moderate and severe water stress levels in Zhao et al. (2020), with consideration from Qaseem et al. (2019) and Giunta et al. (1993). The water stress impacts for other crops are drawn from Sadras et al. (2017). The base data of food supply (FAO, 2020c), and the nutri-

---

[2]The list of vegetables products includes cabbages and other brassicas, artichokes, asparagus, lettuce and chicory, spinach, tomatoes, cauliflowers and broccoli, pumpkins, squash and gourds, cucumbers and gherkins, eggplants (aubergines), chilies and peppers, green, onions, shallots, green, onions, dry, garlic, leeks, other alliaceous vegetables, beans, green, peas, green, vegetables, string beans, carrots and turnips, okra, mushrooms and truffles, vegetables, bananas, plantains and others, oranges, tangerines, mandarins, clementines, satsumas, lemons and limes, grapefruit, fruit, citrus, apples, pears, quinces, apricots, cherries, peaches and nectarines, plums and sloes, stone fruit, strawberries, raspberries, currants, blueberries, berries, grapes, watermelons, melons, other, figs, mangoes, mangosteens, guavas, avocados, pineapples, dates, persimmons, kiwi fruit, papayas, tropical fresh fruit, hops, pepper, chilies and dry peppers (FAO, 2022a).

[3]Livestock (in thousand heads) includes buffaloes, cattle, goats, horses, pigs and sheep. Poultry sectors (in million heads) include chickens, ducks and turkeys.

tional content of foods and grains, are from (FAO, 2020b) and FAO (2020a). The average yearly dietary consumption per capita is from (FAO, 2020a), by country/region. Heat stress indexes are again drawn from Kompas et al. (2018), Kompas and Van Ha (2019) and Roson and Sartori (2016).

6.2 WRI projections of global water stress

The two key recent and most relevant studies of water stress by climate change scenario, particularly in irrigated areas, are Fischer et al. (2007) and WRI (2022a). Within a coherent AEZ framework, Fischer et al. (2007) provides a new methodology for estimating irrigation water requirements under current and future changes by climate and socioeconomic conditions to 2080. In that study, Fischer et al. (2007) projects global and regional agricultural water demand for irrigation using a new socioeconomic scenario developed by IIASA, with and without climate change. Water deficits of crops are projected in the FAO-IIASA-AEZ model, which is based on daily water balances at 0.5^o latitude x 0.5^o longitude and then aggregated to regions and the globe. While the study by Fischer et al. (2007) is valuable for projecting water deficit under the effect of climate change, it is limited to 13 regions (with different regional concordances to GTAP).
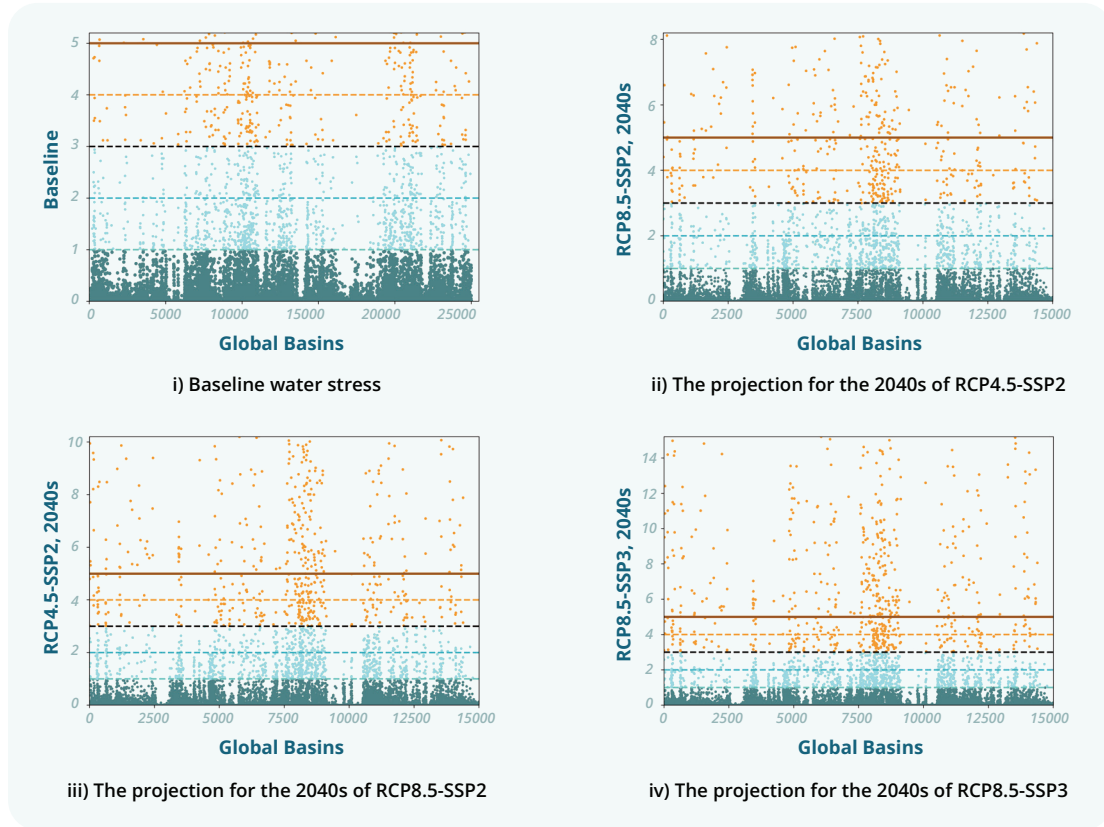
In GTAP-DynW, the shock for water stress is instead based on WRI (2022a), which is extracted from the Geographic Information System (GIS) WRI layers for future water demand, availability and water stress for RCP4.5-SSP2, RCP8.5-SSP2 and RCP8.5-SSP3, covering 15,006 basins for the decadal ranges of the 2020s, 2030s and 2040s (see Luck et al. 2022). We also consider alternative layers for future global water stress and current water data for 25,010 basins from WRI (2022b), and other geographical features from Esri-USGS (2022). Other GIS layers of water and country characteristics are drawn from WRI (2022b) and Esri-USGS (2022).

The WRI water stress projections show the impacts of climate change from global warming in clear terms, with water stress increasing by both the level of water stress and the number of basins moving to higher water stress categories. Using WRI (2022a), we constructed Figure 1 to represent the water stress indexes for the baseline (25,008 basins) and projections of global basins for RCP4.5-SSP2, RCP8.5-SSP2 and RCP8.5-SSP3. WRI (2022a) classified five water stress categories (presented as horizontal lines in Figure 1), including <1: Low water stress; 1-2: Low to Medium water stress; 2-3: Medium to High water stress; 3-4: High water stress; >4: Extremely High water stress. The dark red line represents the case of water stress greater than 5 (or the top limit for the baseline). Following Luck et al. (2022) and WRI (2022a), overall future water stress would increase, given climate change, especially so across a large number of regions, including the Mediterranean, the Middle East, the North American West, Eastern Australia, West Asia, Northern China and Chile. Further details of the WRI projection methodology are presented in Appendix C.

The WRI water projections are provided by decade for the 2020s, 2030s and 2040s. To implement GTAP-DynW, we concentrate on the 15,006 water basins and apply a linear extrapolation to estimate yearly water stress within each decade from 2022 to 2050. From these water stress projections, three steps are required to implement GTAP-DynW by region.

First, the global GIS water data of 15,006 basins is spatially merged with the global GIS layers Esri-USGS (2022) providing a geographical water stress projection for 174 countries, which

Figure 1. Projection of water stress of global basins by climate change scenario

i) Baseline water stress

ii) The projection for the 2040s of RCP4.5-SSP2

iii) The projection for the 2040s of RCP8.5-SSP2

iv) The projection for the 2040s of RCP8.5-SSP3

Source data: Extracted from the GIS spatial layers of WRI (2022a).
Note: Water Stress: <1: Low Water Stress; 1-2: Low to Medium Water Stress; 2-3: Medium to High Water Stress; 3-4: High Water Stress; >4: Extremely High Water Stress. The solid or dark red line indicates water stress >5, the top of the initially indicated water stress limit. Red dots indicate High to Extreme High water stress. Note the change in vertical scale in Figures (i) to (iv), with the index moving to as high as 14, with a substantial increase in the frequency or number of water basins >3 or in the High Water Stress range.

then concord with GTAP-DynW's 30 regions. The water stress at a time by a region i in GTAP-DynW is estimated from the projection of water stress in all basins j located in the region i with a weighted coefficient of j that is measured as the area or share of j in the total basin area in i, or

$$ws(i) = \sum_{j=1}^{J} wsb(i,j) \frac{B(i,j)}{\sum_{j=1}^{J} B(i,j)} \qquad (12)$$

where $wsb(i, j)$ is the water stress of a basin j (in the set J basins located in region i; i belongs to the GTAP-DynW's 30 regions (I); and $B(i, j)$ is the area of basin j located in i.

Second, the time series of water stress by GTAP-DynW region is re-based with the base year as 1.0. Finally, for each crop, the effect of $afw1_{c,j,t}$ is estimated using the effect of the extreme water stress on crop productivity as provided in Sadras et al. (2017) and Zhao et al. (2020) (considering Qaseem et al. (2019) and Giunta et al. (1993)). The impact of other water stress levels is linearly correlated to the impacted levels in these studies. Third, the final shock $dafw1_{c,j,t}$ is adjusted by the share of irrigated area in the total land use of a given crop and/or agricultural output.

6.3 Key limitations

The impacts of climate change on water resources and its impact on agriculture are certainly complex, varying by region, industry and time. Our shocks in GTAP-DynW are based on currently available and up-to-date data, parameters and possible global warming projections. These may change over time and the simulation model will have to be adjusted. There are three limitations that especially need further research.

First, the amount of water by AEZ and regions is estimated from water intensity per hectare by regions, which is derived from AEZ areas and water use by AEZ from Iman et al. (2016). Given the disparity between the 19 regions by Iman et al. (2016) and 30 regions in GTAP-DynW, there is a deviation in baseline water estimates by AEZ in the 30 regions of GTAP-DynW. We have tried to account for this but improving the AEZ water database with more accurate data by regions and agricultural sectors is needed. Second, the parameters for water stress impacts on agricultural production vary by regions and farming industries. The precise water stress impact on each agricultural commodity needs further work by crop and specific agricultural output. We include all that is currently available but more precise and fully articulated impacts would be invaluable. Finally, GTAP-DynW covers a large basket of agricultural commodities aggregated into 14 different types, assumed to be a "basket" of food for nutrition. That is a common procedure. However, some other local food sectors and types (such as in Asia and Africa) are also influenced by water stress but are not available in GTAP or FAO data.

7 Model results

As indicated, GTAP-DynW begins with 141 countries and regions, each with separate baselines for heat and irrigated water stress, aggregated into 30 countries/regions and 30 commodity sectors, with 14 specific agricultural commodity components (see Tables A1 and A2). The water stress measures going forward in time to 2050 are drawn from WRI (2022a), augmented by heat stress (lost agricultural and labour productivity) and other agricultural damage functions. The GTAP model is run with annual resolution to 2050 for three global warming scenarios, RCP4.5-SSP2, RCP8.5-SSP2 and RCP8.5-SSP3, following WRI (2022a). We are agnostic in this report on what RCP is "business-as-usual", with recent work suggesting that although an emissions pathway between RCP4.5 and RCP8.5 is consistent with IEA scenarios, RCP8.5 is still the appropriate scenario to 2050 given tipping points and possible missing biotic feedbacks (Schwalm et al., 2020). An alternative view is offered by Hausfather and Peters (2020). Nevertheless, it is clear that regardless of the chosen RCP heat and water stress have substantial negative impacts.

7.1 Agricultural production

Tables 2–4 summarise the results of selected global agricultural commodities by climate change scenario. The fall in agricultural production increases from RCP4.5 to RCP8.5 and from RCP8.5-SSP2 to RCP-SSP3. The tables indicate annual time steps and both average annual growth rates and the fall in output from 2024 to 2050. The baseline is 2020 as drawn from FAO (2022a). Paddy is impacted the most, but all outputs fall in global terms.

Table 2. Global agricultural production of RCP4.5 scenario

Year	Agricultural Supply								
	Paddy	Wheat	Cereal	Veggie	Oilseed	Othe Crops	Live stock	AnimPrd	Dairy
	Mt	Mt	Mt	Mt	Mt	Mt	Mheads	Mt	Mt
2024	735,411	720,262	1,330,584	2,799,439	845,032	61,206	4,820	1,685,429	812,032
2025	732,487	719,243	1,330,137	2,798,593	844,923	61,181	4,810	1,682,403	811,135
2026	729,555	718,241	1,329,703	2,797,744	844,807	61,157	4,800	1,679,349	810,205
2027	729,555	718,241	1,329,703	2,797,744	844,807	61,157	4,800	1,679,349	810,205
2028	723,693	716,304	1,328,844	2,795,960	844,556	61,103	4,779	1,673,136	808,322
2029	720,751	715,371	1,328,452	2,794,975	844,408	61,075	4,769	1,669,971	807,335
2030	717,774	714,478	1,327,910	2,793,986	844,157	61,040	4,758	1,666,838	806,315
2031	714,767	713,604	1,327,375	2,792,970	843,907	61,003	4,748	1,663,697	805,265
2032	711,776	712,759	1,326,857	2,791,946	843,646	60,966	4,737	1,660,477	804,211
2033	708,772	711,917	1,326,328	2,790,895	843,345	60,928	4,726	1,657,251	803,129
2034	705,741	711,097	1,325,841	2,789,836	843,029	60,889	4,715	1,653,946	802,016
2035	702,719	710,288	1,325,372	2,788,762	842,706	60,850	4,704	1,650,622	800,900
2036	699,673	709,492	1,324,903	2,787,583	842,375	60,810	4,694	1,647,262	799,763
2037	696,636	708,706	1,324,444	2,786,381	842,025	60,768	4,682	1,643,828	798,603
2038	693,576	707,921	1,323,989	2,785,165	841,666	60,726	4,671	1,640,381	797,428
2039	690,504	707,171	1,323,561	2,783,941	841,276	60,683	4,660	1,636,862	796,234
2040	686,865	706,227	1,322,138	2,781,428	840,016	60,581	4,645	1,631,570	794,077
2041	683,211	705,322	1,320,729	2,778,902	838,753	60,479	4,631	1,626,200	791,902
2042	679,173	704,200	1,319,065	2,776,241	837,493	60,376	4,616	1,620,447	789,607
2043	675,142	703,124	1,317,446	2,773,585	836,190	60,271	4,601	1,614,681	787,299
2044	671,099	702,087	1,315,843	2,770,917	834,874	60,166	4,585	1,608,903	784,971
2045	667,072	701,098	1,314,273	2,768,217	833,545	60,062	4,569	1,603,053	782,626
2046	663,035	700,148	1,312,726	2,765,510	832,224	59,958	4,554	1,597,192	780,266
2047	658,985	699,237	1,311,214	2,762,778	830,887	59,855	4,538	1,591,335	777,882
2048	654,942	698,367	1,309,716	2,760,021	829,552	59,750	4,522	1,585,401	775,491
2049	650,876	697,539	1,308,256	2,757,253	828,212	59,645	4,506	1,579,454	773,076
2050	646,854	696,763	1,306,887	2,754,491	826,952	59,545	4,490	1,573,626	770,736
Average Annual Growth Rate (%)									
	-0.49	-0.13	-0.07	-0.06	-0.08	-0.10	-0.27	-0.26	-0.20
Change between 2024 and 2050 (%)									
	-12.04	-3.26	-1.78	-1.61	-2.14	-2.71	-6.85	-6.63	-5.09

Table 3. Global agricultural production of RCP8.5-SSP2 scenario

Year	Agricultural Supply								
	Paddy	Wheat	Cereal	Veggie	Oilseed	Other-Crops	Live-stock	AnimPrd	Dairy
	Mt	Mt	Mt	Mt	Mt	Mt	Mheads	Mt	Mt
2024	736,291	720,004	1,329,855	2,799,101	844,578	61,176	4,815	1,684,602	811,500
2025	733,432	718,744	1,328,967	2,798,110	844,313	61,138	4,803	1,681,114	810,359
2026	730,441	717,426	1,328,041	2,797,070	844,010	61,099	4,790	1,677,482	809,171
2027	727,331	716,040	1,327,035	2,795,962	843,703	61,057	4,777	1,673,709	807,916
2028	724,073	714,586	1,325,919	2,794,813	843,358	61,012	4,764	1,669,785	806,625
2029	720,698	713,052	1,324,737	2,793,610	843,002	60,965	4,750	1,665,667	805,278
2030	717,144	711,469	1,323,384	2,792,295	842,568	60,914	4,735	1,661,402	803,873
2031	713,456	709,811	1,321,971	2,790,916	842,101	60,860	4,720	1,656,986	802,416
2032	709,615	708,087	1,320,470	2,789,496	841,612	60,804	4,705	1,652,423	800,903
2033	705,600	706,269	1,318,868	2,787,976	841,122	60,744	4,688	1,647,643	799,337
2034	701,436	704,365	1,317,160	2,786,400	840,598	60,683	4,672	1,642,701	797,693
2035	697,103	702,366	1,315,356	2,784,763	840,032	60,620	4,655	1,637,584	795,980
2036	692,597	700,273	1,313,457	2,783,067	839,441	60,553	4,637	1,632,238	794,210
2037	687,932	698,072	1,311,414	2,781,271	838,847	60,483	4,618	1,626,665	792,380
2038	683,051	695,758	1,309,263	2,779,404	838,218	60,411	4,599	1,620,926	790,461
2039	677,975	693,329	1,306,971	2,777,462	837,575	60,336	4,579	1,614,957	788,481
2040	672,208	690,553	1,304,047	2,773,593	836,323	60,196	4,557	1,607,792	785,996
2041	666,254	687,704	1,301,035	2,769,628	835,033	60,055	4,533	1,600,388	783,430
2042	659,370	684,295	1,297,381	2,765,544	833,718	59,906	4,507	1,592,075	780,587
2043	652,264	680,787	1,293,588	2,761,476	832,381	59,754	4,480	1,583,509	777,647
2044	644,933	677,184	1,289,662	2,757,292	831,031	59,600	4,453	1,574,689	774,617
2045	637,392	673,491	1,285,613	2,752,989	829,665	59,443	4,424	1,565,600	771,497
2046	629,621	669,687	1,281,401	2,748,598	828,271	59,282	4,395	1,556,198	768,269
2047	621,612	665,763	1,277,069	2,744,181	826,848	59,119	4,365	1,546,471	764,950
2048	613,360	661,726	1,272,588	2,739,668	825,416	58,953	4,333	1,536,479	761,516
2049	604,889	657,556	1,267,932	2,735,075	823,988	58,784	4,301	1,526,149	757,988
2050	596,215	653,273	1,263,147	2,730,639	822,607	58,619	4,268	1,515,583	754,379
Average Annual Growth Rate (%)									
	-0.78	-0.36	-0.19	-0.09	-0.10	-0.16	-0.45	-0.39	-0.27
Change between 2024 and 2050 (%)									
	-19.02	-9.27	-5.02	-2.45	-2.60	-4.18	-11.36	-10.03	-7.04

Table 4. Global agricultural production of RCP8.5-SSP3 scenario

Year	Agricultural Supply								
	Paddy	Wheat	Cereal	Veggie	Oilseed	Other Crops	Live-stock	Animal Prd	Dairy
	Mt	Mt	Mt	Mt	Mt	Mt	Mheads	Mt	Mt
2024	736,107	719,864	1,329,681	2,799,064	844,538	61,176	4,815	1,684,371	811,434
2025	733,004	718,452	1,328,657	2,797,998	844,273	61,137	4,802	1,680,651	810,237
2026	729,686	716,906	1,327,525	2,796,867	843,978	61,095	4,788	1,676,742	808,955
2027	726,150	715,228	1,326,221	2,795,696	843,660	61,050	4,774	1,672,599	807,604
2028	722,373	713,408	1,324,741	2,794,447	843,315	61,003	4,759	1,668,195	806,174
2029	718,323	711,455	1,323,133	2,793,196	842,957	60,953	4,743	1,663,516	804,665
2030	713,986	709,346	1,321,257	2,791,808	842,505	60,898	4,727	1,658,650	803,069
2031	709,367	707,065	1,319,205	2,790,351	842,029	60,840	4,709	1,653,490	801,379
2032	704,469	704,616	1,316,964	2,788,808	841,515	60,779	4,691	1,647,983	799,602
2033	699,228	701,964	1,314,514	2,787,244	840,978	60,715	4,672	1,642,181	797,699
2034	693,677	699,122	1,311,844	2,785,582	840,412	60,647	4,652	1,636,026	795,699
2035	687,783	696,061	1,308,928	2,783,850	839,827	60,576	4,630	1,629,555	793,597
2036	681,551	692,771	1,305,737	2,782,048	839,234	60,502	4,608	1,622,698	791,359
2037	674,935	689,224	1,302,285	2,780,154	838,614	60,424	4,584	1,615,455	788,993
2038	667,939	685,420	1,298,556	2,778,134	837,949	60,344	4,560	1,607,759	786,505
2039	660,540	681,349	1,294,516	2,776,102	837,273	60,260	4,534	1,599,649	783,863
2040	652,214	676,712	1,289,667	2,772,088	835,982	60,110	4,504	1,590,141	780,670
2041	643,476	671,801	1,284,484	2,768,025	834,673	59,956	4,473	1,580,156	777,318
2042	633,220	665,856	1,278,158	2,763,755	833,318	59,794	4,438	1,568,701	773,518
2043	622,498	659,576	1,271,424	2,759,436	831,950	59,627	4,401	1,556,676	769,530
2044	611,275	652,948	1,264,251	2,755,023	830,578	59,457	4,363	1,544,084	765,352
2045	599,563	645,954	1,256,625	2,750,525	829,191	59,283	4,322	1,530,831	760,980
2046	587,369	638,572	1,248,575	2,745,955	827,783	59,106	4,280	1,516,918	756,394
2047	574,664	630,786	1,239,988	2,741,394	826,360	58,926	4,236	1,502,332	751,592
2048	561,468	622,605	1,230,892	2,736,760	824,941	58,742	4,190	1,487,079	746,546
2049	547,790	614,000	1,221,277	2,731,997	823,518	58,555	4,142	1,471,043	741,268
2050	533,662	604,996	1,211,170	2,727,412	822,140	58,370	4,092	1,454,337	735,783
Average Annual Growth Rate (%)									
	-1.17	-0.63	-0.34	-0.10	-0.11	-0.18	-0.60	-0.54	-0.36
Change between 2024 and 2050 (%)									
	-27.50	-15.96	-8.91	-2.56	-2.65	-4.59	-15.00	-13.66	-9.32

In particular, the decline in production at an average annual rate for RCP4.5-SSP2, RCP8.5-SSP2 and RCP8.5-SSP3 is -0.49, -0.78 and -1.17% for paddy; -0.13, -0.36 and -0.63% for wheat; -0.07, -0.19, -0.34% for cereal; -0.06, -0.09 and -0.10% for vegetables; -0.08, -0.10 and -0.11% for oilseed; -0.10, -0.16 and -0.18% for other crops; -0.27, -0.45 and -0.60% for livestock; -0.26, -0.39 and -0.54% for animal products; and finally -0.20, -0.27 and -0.36% for dairy.

From 2024 to 2050, for RCP4.5, RCP8.5-SSP2 and RCP8.5-SSP3, global output falls by 12.04%, 19.02% and 27.05% for paddy; 3.26%, 9.27% and 15.96% for wheat; 1.78%, 5.02% and 8.91% for cereal; 1.61%, 2.45% and 2.56% for vegetables; 2.14%, 2.60% and 2.65% for oilseed; 2.71%, 4.18% and 4.59% for other crops; 6.85%, 11.36% and 15.00% for livestock; 6.63%, 10.03% and 13.66% for animal products; 5.09%, 7.04% and 9.32% for dairy.

Figures 2 and 3 summarise the production path or output losses to 2050 by climate change scenario for paddy, wheat, cereal, oilseed, vegetables, livestock, meat and dairy, across different parts of the world. Overall, agricultural output falls to the year 2050 under the impact of climate change; the higher the global warming level, the more negative the impact on agricultural production. Exceptional cases are for wheat and cereals in some areas with RCP4.5, in particular, where yields are better off in some countries (such as Canada, New Zealand, Austria, Belgium, France, Germany, Russia and Ukraine). By group level, ROW's cereal output increases slightly with RCP4.5-SSP2 and RCP8.5-SSP2. For RCP8.5-SSP3, however, the impact of climate change is consistently negative for all sectors and areas. The most affected industries from global warming worldwide are paddy, wheat, cereal, livestock, meat (animal products) and dairy.

Figure 2. Production to 2050 of paddy, wheat, cereal and oilseed
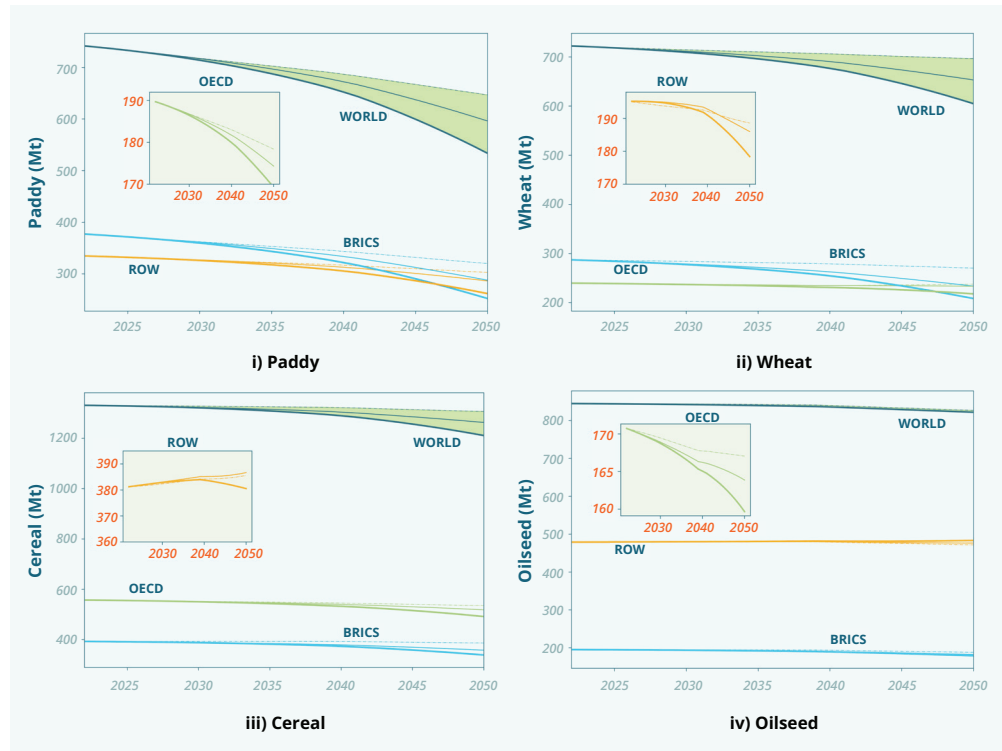
Note: GTAP-DynW model output. (- [dotted]), (–) and (– [bold]) present for the scenario of RCP4.5; RCP8.5-SSP2 and RCP8.5-SSP3, respectively. Results with water and heat stress under different climate change scenarios. Note the change in scale in the box inserts.

Figure 3. Production to 2050 of vegetables, livestock, meat and dairy
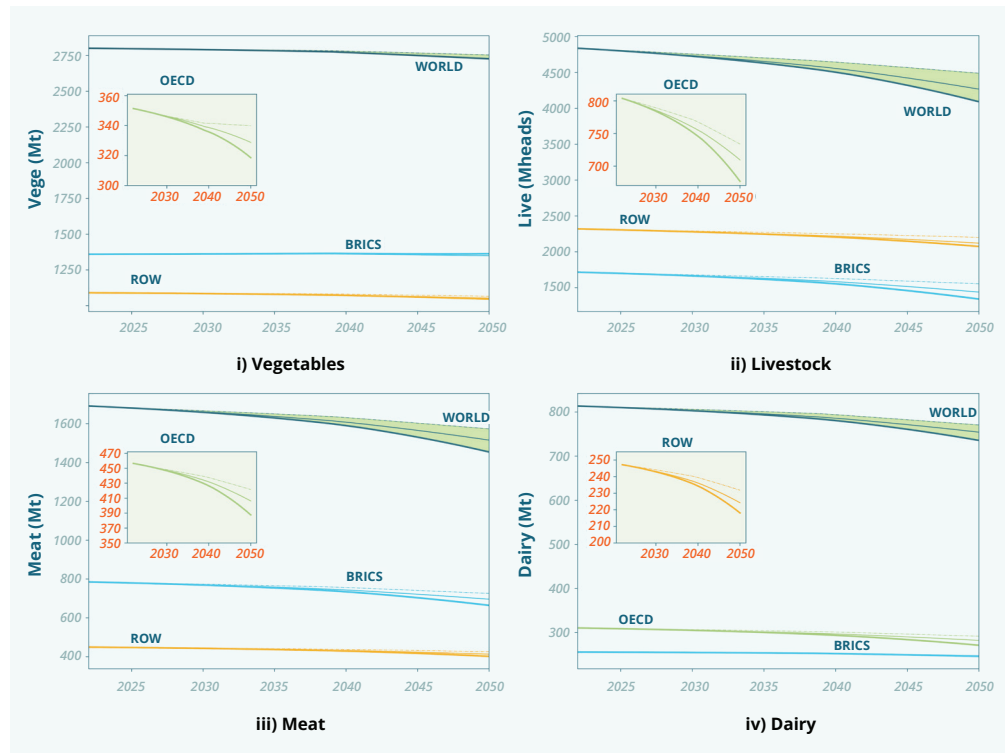
i) Vegetables

ii) Livestock

iii) Meat

iv) Dairy

Note: GTAP-DynW model output. (- [dotted]), (–) and (– [bold]) present for the scenario of RCP4.5; RCP8.5-SSP2 and RCP8.5-SSP3, respectively. Results with water and heat stress under different climate change scenarios. Note the change in scale in the box inserts.

7.2 Food supply

Food supply is aggregated as total nutrition by thousand Giga-calories (thous Gcal) as given in equation (8), using nutritional conversion factors for the total supply of food across all commodity sectors. A decrease in agricultural outputs would thus cause a reduction in the global food supply (measured in total energy for nutrition) and an increasing number of people (millions) losing food security. GTAP-DynW provides these measures as model output for all climate change scenarios. The base year is 2020, drawn from FAO (2022a).

In the global map, Figures 4–6 show a decreasing trend of food supply as % reduction in 2050 from the base year by climate change scenario. The global food supply falls by 5.8%, 9.7% and 14.2% on average for RCP4.5-SSP2, RCP8.5-SSP2 and RCP8.5-SSP3, respectively.

For RCP4.5, the food supply decreases by 5.1–6.6% in Africa, 5.8% for Australia and 6.4% for some parts of South America. In 2050, for this scenario, food supply falls by 4.8% for the US, 8.97% for China and 6.52% for India. However, for RCP8.5-SSP3, the worst-case scenario, food supply decreases by 8.2–11.8% in Africa, 14.7% for Australia and 19.4% for some parts of Central America. For this scenario, in 2050, the food supply would fall by 12.6% for the US, 22.4% for China and 16.1% for India.

Figure 4. Reduction of global food supply from irrigated water and heat stress at RCP4.5 in 2050 (% ranges)
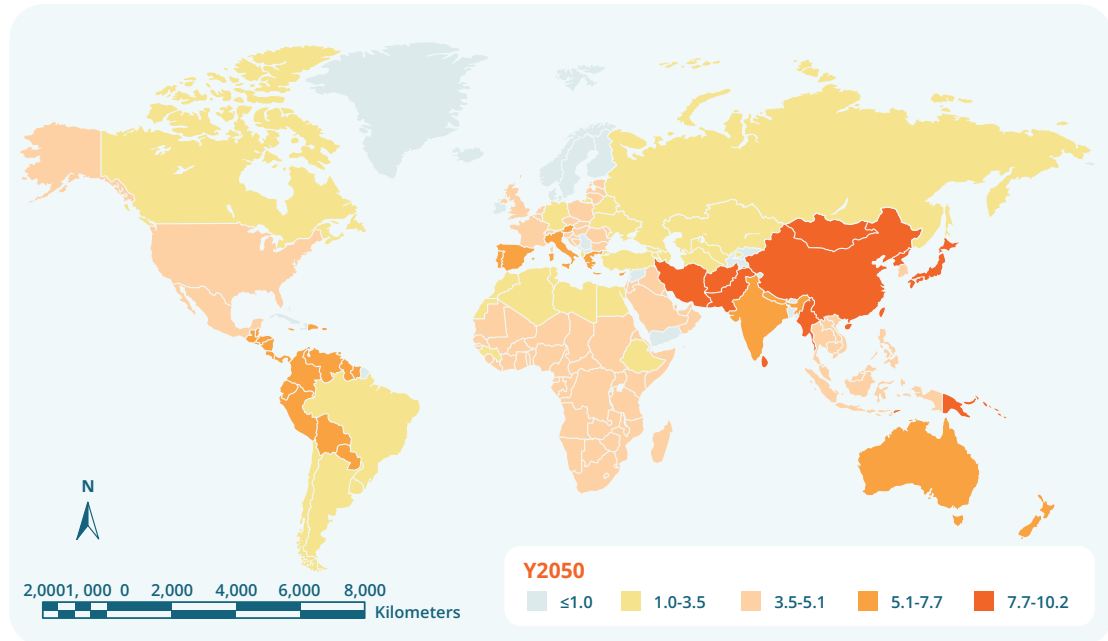
Y2050
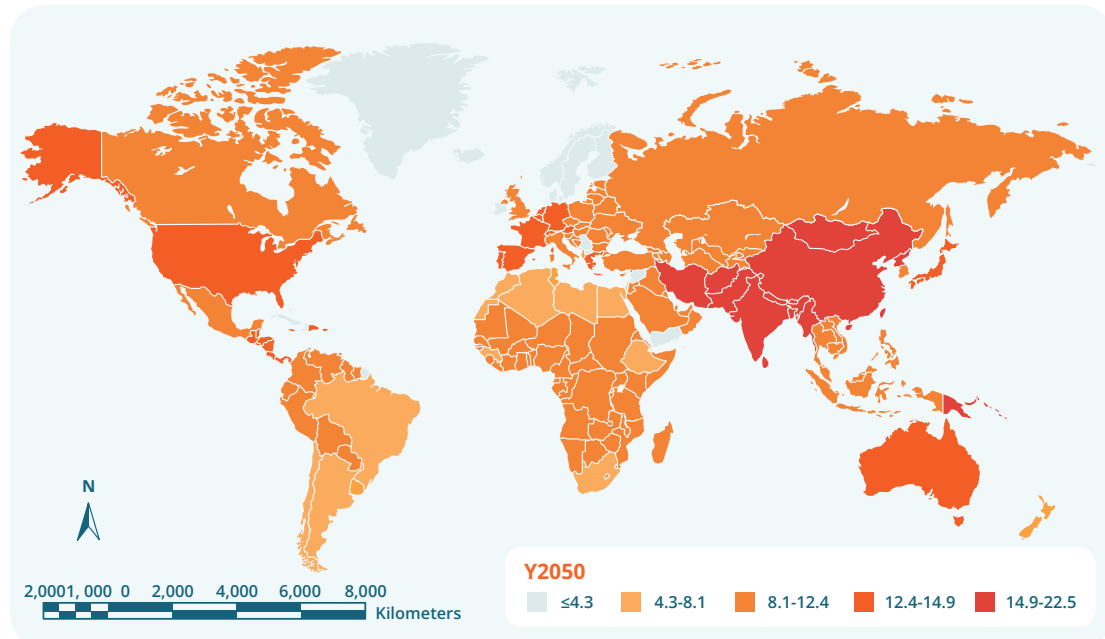≤1.0 | 1.0-3.5 | 3.5-5.1 | 5.1-7.7 | 7.7-10.2

Note: GTAP-DynW model output, showing % reduction in food supply using a calorie metric. (i) Food supply is aggregated as total nutrition by trillion calories; Food reduction (% ranges) is compared with the base year of 2020 drawn from FAO (2022a).

Figure 5. Reduction of global food supply from irrigated water and heat stress at RCP8.5- SSP2 in 2050 (% ranges)
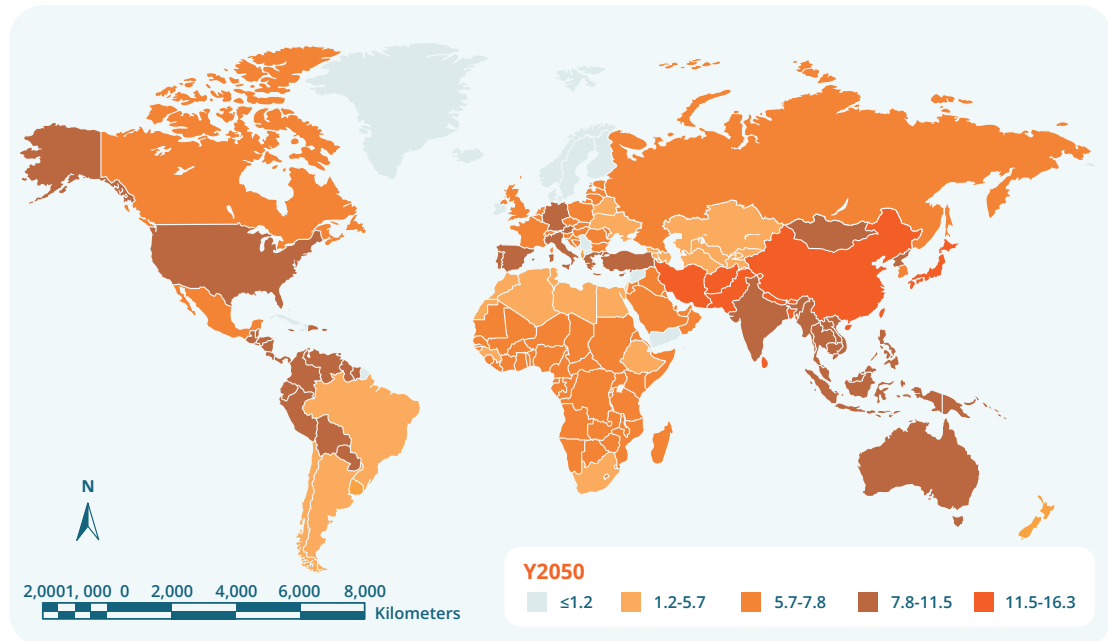
Y2050
≤1.2 | 1.2-5.7 | 5.7-7.8 | 7.8-11.5 | 11.5-16.3

Note: GTAP-DynW model output, showing % reduction in food supply using a calorie metric.
(i) Food supply is aggregated as total nutrition by trillion calories; ii) Food reduction (% ranges) is compared with the base year of 2020 drawn from FAO (2022a).

Figure 6. Reduction of global food supply from irrigated water and heat stress at RCP8.5- SSP3 in 2050 (% ranges)
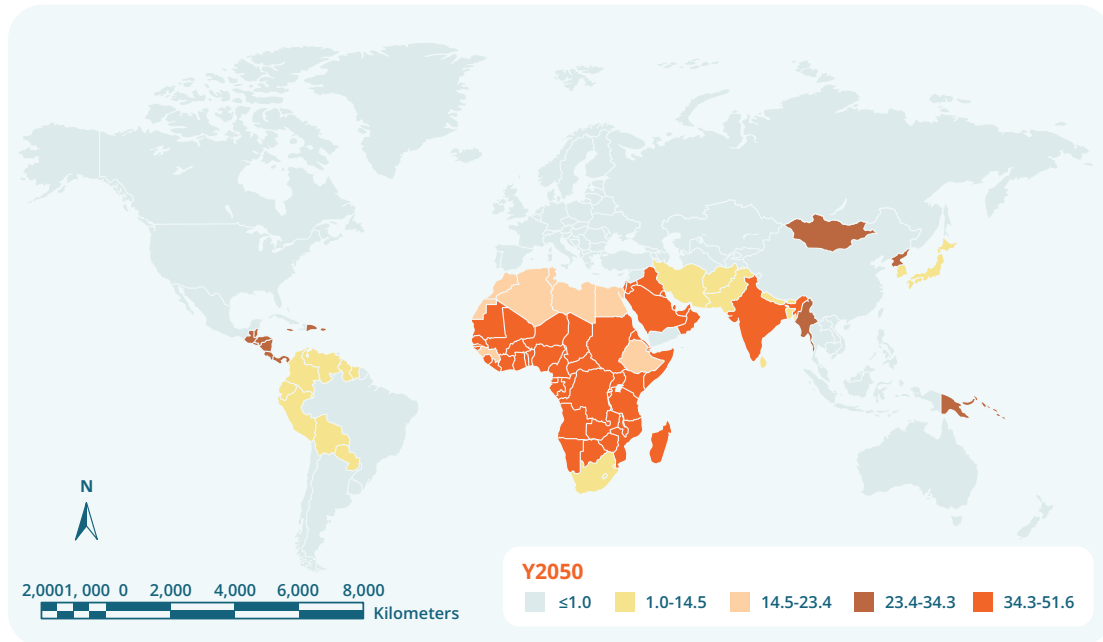

Note: GTAP-DynW model output, showing % reduction in food supply using a calorie metric. (i) Food supply is aggregated as total nutrition by trillion calories; Food reduction (% ranges) is compared with the base year of 2020 drawn from FAO (2022a).

7.3 Food security

The number of "food insecure" persons (millions) resulting from the decrease in food supply (or aggregated nutritional supply) is estimated following equation (8), as a measure of the reduction in food supply relative to base nutritional supply. All outputs are trade-adjusted noting that many countries are net food exporters so a fall in food supply will not impact food insecurity for that population (although domestic prices vary considerably). As indicated, the number of people facing food insecurity in a region is calculated by dividing the reduction of food supply (thous GCal) by the average dietary needs for a million people per year (in calories) in that country or region (source baseline data: FAO (2020c), FAO (2020b) and FAO (2020a)). Population growth in GTAP-DynW in 2050 is based on World Bank (2020).

Water and stress from climate change causes global food insecurity to increase overall (see Figures 7–9). Despite a fall in food supply, some current net food exporters (such as Australia, the USA, Germany, France and Russia) remain secure in potentially meeting their domestic needs for food demand. However, many regions, especially LDCs, will face food insecurity. For example, in 2050, for RCP8.5-SSP3, the domestic supply in many African countries only meets 42.3% of domestic demand, leaving 57.6% of the population facing food insecurity (see Figure 9). Some areas, such as China and ASEAN, will switch from a food security status to becoming net food importers in 2050. Figures 7 to 9 present global maps of food insecurity in 2050. Overall, Africa is the most critical area under threat of food insecurity, particularly due to heat stress, but countries in the Middle East, South Asia and Central America (among others) are also badly impacted.

Figure 7. Global food insecurity of RCP4.5 in 2050 (%)

Y2050

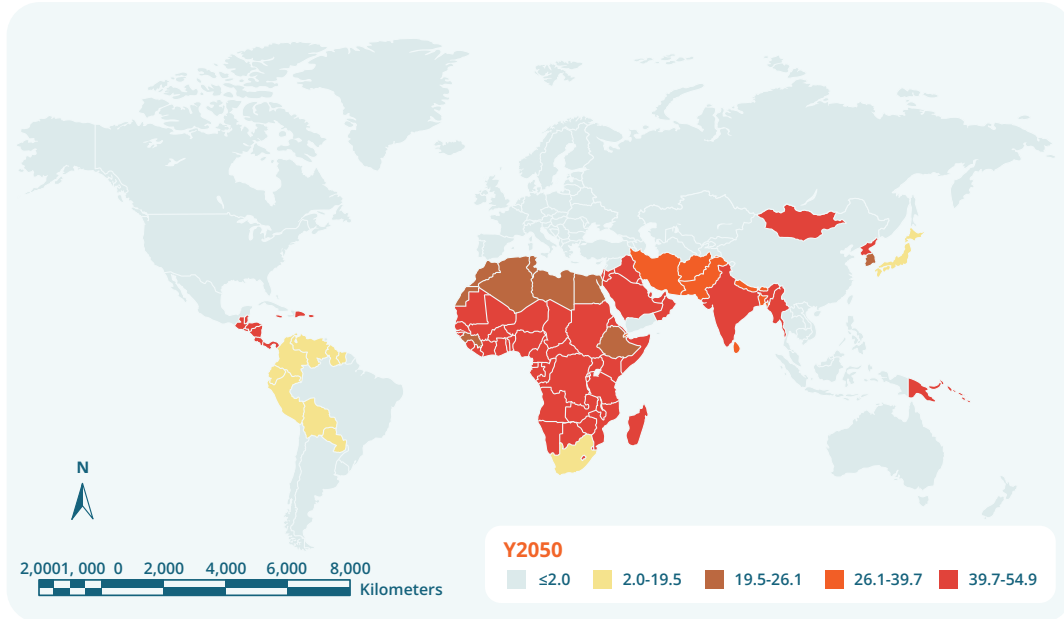|				
≤1.0	1.0-14.5	14.5-23.4	23.4-34.3	34.3-51.6

Note: GTAP-DynW model output, showing the percentage of the population that is food insecure, from irrigated water and heat stress, additional to the 2020 baseline. Food insecurity is measured as a % of the shortage from the domestic supply for food to meet average nutritional demands of the population in the country or region. (Source for nutritional baseline data: FAO (2020c), FAO (2020b) and FAO (2020a))

Figure 8. Global food insecurity of RCP8.5-SSP2 in 2050 (%)
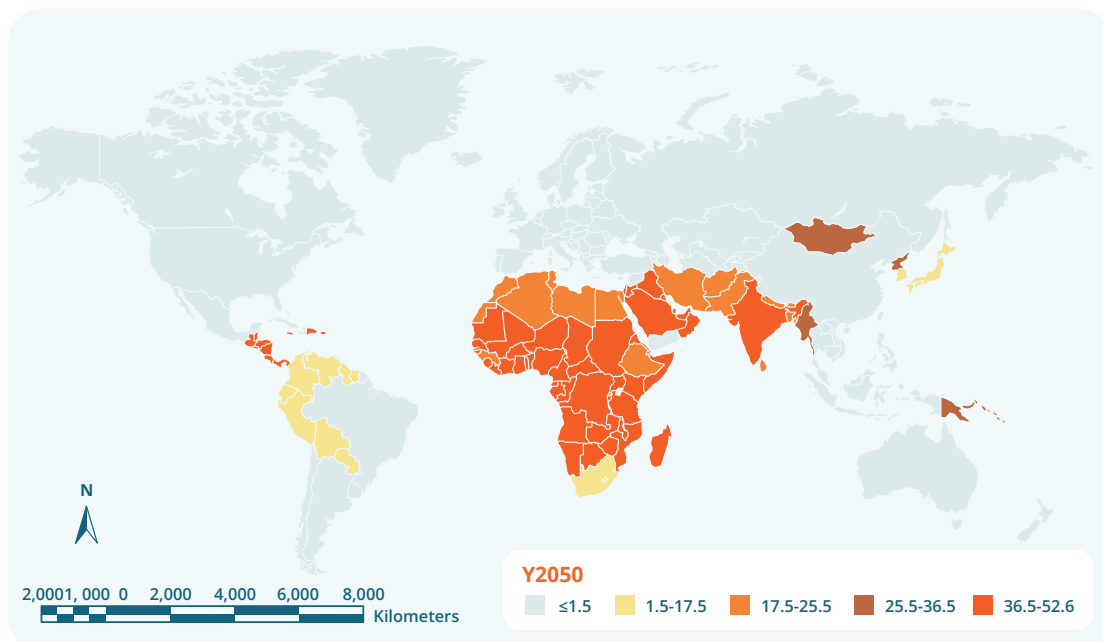
Y2050

≤1.5	1.5-17.5	17.5-25.5	25.5-36.5	36.5-52.6

Note: GTAP-DynW model output, showing the percentage of the population that is food insecure, from irrigated water and heat stress, additional to the 2020 baseline. Food insecurity is measured as a % of the shortage from the domestic supply for food to meet average nutritional demands of the population in the country or region. (Source for nutritional baseline data: FAO (2020c), FAO (2020b) and FAO (2020a)).

Figure 9. Global food insecurity of RCP8.5-SSP3 in 2050 (%)

Note: GTAP-DynW model output, showing the percentage of the population that is food insecure, from irrigated water and heat stress, additional to the 2020 baseline. Food insecurity is measured as a % of the shortage from the domestic supply for food to meet average nutritional demands of the population in the country or region. (Source nutritional baseline data: FAO (2020c), FAO (2020b) and FAO (2020a)).

These food insecurity results can be translated into numbers of individuals. Figure 10 presents global food supply (measured in total energy nutrition) and the number of food insecure people (million persons) resulting from the decline of the food supply over time. All three cases are indicated: RCP4.5, RCP8.5-SPP2 (A) and RCP8.5-SSP3 (B). In 2050, the global food supply decreases continuously from 9.75 million to 9.2, 8.8 and 8.4 million Gcal (the left axis) and the resulting and equivalent the nutritional shortage in terms of food insecure persons, compared to base 2020, increases from 556 million to 935 million and 1.36 billion people (the right axis) for RCP4.5-SSP2, RCP8.5-SSP2 (A) and RCP8.5-SSP3 (B), respectively.

Figure 10. Global food supply (Gcal) and food insecurity (Mill pers)
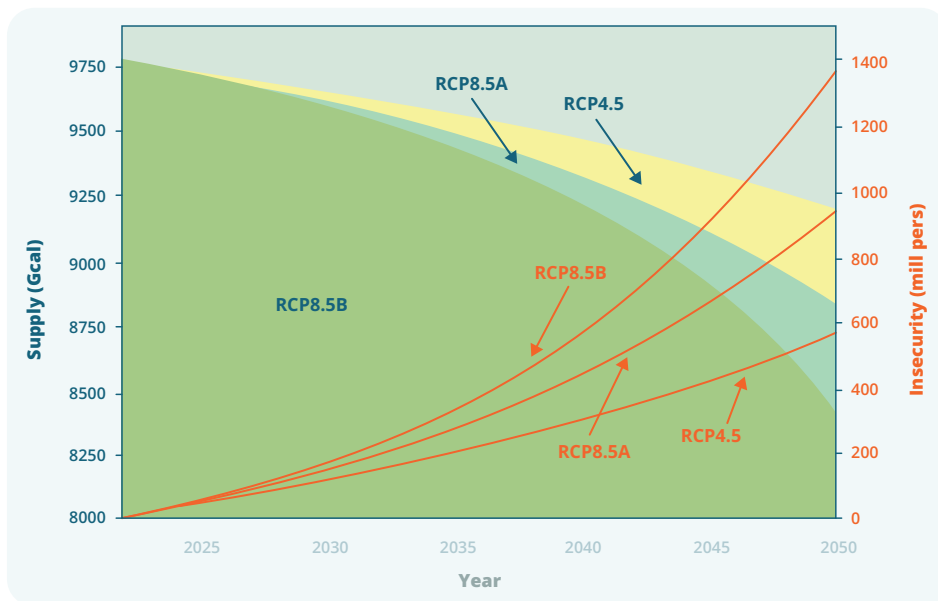
Note: GTAP-DynW model output. RCP8.5A is RCP8.5-SSP2 and RCP8.5B is the RCP8.5- SSP3 scenario. Green areas and blue letters represent food supply (left axis); red lines and red notes are for food insecurity (right axis). Baseline is 2020.

8 Closing remarks

The impacts of water stress due to global warming and its impact on agriculture are complex and vary by region, commodity sector and time. This technical report presented a large-dimensional climate and trade model, GTAP-DynW, to project the impacts of irrigated water and heat stress by climate change scenario on agricultural production, total food supply and food security to 2050. The results are striking, indicating substantial falls (using a calorie metric) in overall global food supply of 5.8%, 9.7% and 14.2% to 2050, with a resulting nutritional shortage or "food insecurity" for 556 million, 935 million and 1.36 billion additional people, compared to a 2020 baseline, for RCP4.5-SSP2, RCP8.5-SSP2 and RCP8.5-SSP3 respectively. Results are also indicated for individual commodities with paddy, wheat, cereal, livestock, meat (animal products) and dairy the most impacted, or with the largest losses in agricultural output.

Along with the limitations already indicated in the main report, several further considerations should also be addressed. The projection of water stress in this report is for blue water only, but the role of effective rain-fed (or green water) management is still important and could help increase resilience to global climate change. According to Rockström et al. (2009), many countries currently assessed as having severe water shortages may meet the population demand for food by improving the effective management of green water. However, the combination of both water and heat stress may qualify this view.

The role of groundwater storage is also important for water users. Using the land surface models (LSMs) and the GRACE data from the Gravity Recovery and Climate Experiment, Shamsudduha and Taylor (2020) investigates changes in groundwater storage in the world's 37 large aquifer systems from 2002 to 2016. The study shows that changes in groundwater storage continue to be highly uncertain, especially so changes in other terrestrial stores of water found in soil, surface water and snow/ice (Shamsudduha and Taylor, 2020). Improving groundwater storage management could help increase resilience to water stress due to climate change.

Finally, given the lack of projections on water quality by climate change, the change in water quality with irrigation is not considered. According to Scanlon et al. (2007), increased water irrigation could cause mobilisation of salts and salinisation that severely impact water tables. In addition, with irrigation, fertiliser can leach into underlying aquifers and discharge to streams. Also, irrigation based on surface water can reduce streamflow and raise water tables, causing water-logging (decreasing oxygen to root systems), as evident in many areas (China, India and United States) in the last few decades (Scanlon et al., 2007).

9 References

Aguiar, A. et al. (2019), "The GTAP data base: Version 10", *Journal of Global Economic Analysis,* Vol. 4/1, pp. 1–27.

Ahmed, S. et al. (2016a), *GTAP-AEZ: Land Use Application of the GTAP Mode*, Purdue University, www.gtap.agecon.purdue.edu.

Ahmed, S. et al. (2016b*), Presentation of GTAP-AEZ, GTAP Presentation*, www.gtap.agecon. purdue.edu.

Bellie, S. (2011), "Global climate change and its impacts on water resources planning and management: assessment and challenges", *Stochastic Environmental Research and Risk Assessment,* Vol. 25, pp. 583–600.

Burniaux, J.-M. and T. Truong (2002), "GTAP-E: An energy-environmental version of the GTAP model", *GTAP Technical Paper* 16.

Calvin, K. et al. (2019), "GCAM v5.1: representing the linkages between energy, water, land, climate, and economic systems", *Geoscientific Model Development,* Vol. 12/2, pp. 677–698, https://gmd.copernicus.org/articles/12/677/2019/.

Chepeliev, M. (2020), "GTAP-Power 10a database: a technical note", *Research Memorandum No. 31*, https://gtap.agecon.purdue.edu.

Covey, C. (2003), "An overview of results from the coupled model inter-comparison project (CMIP)", *Program for Climate Model Diagnosis & Intercomparison*, https://pcmdi.llnl.gov/mips/cmip/

Dolan, F. et al. (2017), "Ground- water depletion embedded in international food trade", *Nature,* 543, pp. 700–704.

Dolan, F. et al. (2021), "Evaluating the economic impact of water scarcity in a changing world", *Nature Communications,* 12, pp. 1–9.

EEA (2022), *Water Stress*, European Environment Agency (EEA), EEA Glossary, www.eea.europa.eu/.

Esri-USGS (2022), "ArcGIS data store", *ArcGIS Enterprise*, https://hub.arcgis.com/datasets/.

FAO (2019), *Water Scarcity – One of the Greatest Challenges of our Time*, Food and Agriculture Organization, Rome.

FAO (2020a), *Average Daily Dietary Energy Consumption Per Capita*, Food and Agriculture Organization, Rome

FAO (2020b), *Calculation of the Energy Contents of foods- Energy Conversion Factors*, Food and Agriculture Organization, Rome

FAO (2020c), "FAO stats", Food and Agriculture Organization, Rome, www.fao.org/faostat/en/.

FAO (2020d), "Food Security", Food and Agriculture Organization, Rome, www.fao.org/file-admin/templates/.

FAO (2022a), "FAO Statistics", Food and Agriculture Organization, Rome, www.fao.org/faostat/en/data.

FAO (2022b), "GAEZ: Global Agro-Ecological Zones", Food and Agriculture Organization, Rome, www.fao.org/nr/gaez/en.

Fecht, S. (2019), "How Climate Change Impacts Our Water", Columbia Climate School, https://news.climate.columbia.edu/.

Fischer, G. et al. (2007), "Climate change impacts on irrigation water requirements: Effects of mitigation, 1990–2080", *Technological Forecasting and Social Change,* Vol. 74/7, pp. 1083–1107.

Gassert, F. et al. (2014), *Aqueduct Global Maps 2.1*, Working Paper, World Resources Institute, Washington, DC, www.wri.org/publication/aqueduct-metadata-global.

Giunta, F., R. Motzo and M. Deidda (1993), "Effect of drought on yield and yield components of durum wheat and triticale in a Mediterranean environment", *Field Crops Research,* Vol. 33/4, pp. 399–409, www.sciencedirect.com/science/article/pii/037842909390161F.

Grafton, Q., J. Williams and Q. Jiang (2017), "Possible pathways and tensions in the food and water nexus", *Earth's Future,* Vol. 5, pp. 449–462.

GTAP (2021), "GTAP (Global Trade Analysis Project)", Global Trade Analysis Project. www.gtap.agecon.purdue.edu/.

Hausfather, Z. and G.P. Peters (2020), "Rcp8. 5 is a problematic scenario for near-term emissions", *Proceedings of the National Academy of Sciences,* Vol. 117/45, pp. 27791–27792.

Hertel, T.W. (ed.) (1997), *Trade Analysis: Modeling and Applications*, Cambridge University Press, Cambridge, New York.

IIASA (2019), SSP Database (Shared Socioeconomic Pathways) - Version 2.0, International Institute for Applied Systems Analysis, online, https://tntcat.iiasa.ac.at/SspDb, accessed on 12 March 2019.

Iman, H. et al. (2016), "Introducing irrigation water into GTAP 9 data base", *GTAP Resources 5168*, www.gtap.agecon.purdue.edu.

Kompas, T., V.H. Pham and T.N. Che (2018), "The effects of climate change on GDP by country and the global economic gains from complying with the Paris Climate Accord", *Earth's Future,* Vol. 6/8, pp. 1153–1173.

Kompas, T. and P. Van Ha (2019), "The 'curse of dimensionality' resolved: The effects of climate change and trade barriers in large dimensional modelling", *Economic Modelling,* Vol. 80, pp. 103–110.

Lee, H.-L. (2004), "Incorporating agro-ecologically zoned land use data and landbased greenhouse gases emissions into the GTAP framework", *Research Publication*, www.researchgate.net/publication.

Luck, M., M. Landis and F. Gassert (2022), Aqueduct Water Stress Projections: Decadal Projections of Water Supply and Demand Using CMIP5 GCMs', World Resources Institute, https://resourcewatch.org/data/.

Müller Schmied, H. et al. (2021), "The global water resources and use model WaterGap v2.2d: Model description and evaluation", *Geoscientific Model Development,* Vol. 14/2, pp. 1037–1079, https://doi.org/10.5194/gmd-14-1037-2021.

Piontek, F. et al. (2021), "Integrated perspective on translating biophysical to economic impacts of climate change", *Nature Climate Change,* Vol. 11/7, pp. 563–572.

Plevin, R. et al. (2014), *Agro-ecological Zone Emission Factor (AEZ-EF) Model-V47*, Purdue University, www.gtap.agecon.purdue.edu.

Pérez-Escamilla, R. (2017), "Food security and the 2015–2030 sustainable development goals: From human to planetary health: Perspectives and opinions", *Current Developments in Nutrition,* Vol. 1/7, e000513, https://doi.org/10.3945/cdn.117.000513

Qaseem, M.F., R. Qureshi and H. Shaheen (2019), Effects of pre-anthesis drought, heat and their combination on the growth, yield and physiology of diverse wheat *(Triticum aestivum* L.*)* genotypes varying in sensitivity to heat and drought stress, *Nature Briefing,* Vol. 9/1, pp. 1–12.

Ritchie, H. and M. Roser (2022), Water Use and Stress, Our World in Data, https://ourworldin-data.org.

Rockström, J. et al. (2009), Future water availability for global food production: The potential of green water for increasing resilience to global change, *Water Resources Research,* Vol. 45, pp. 1–16.

Roson, R. and M. Sartori (2016), "Estimation of climate change damage functions for 140 regions in the GTAP 9 database", *Journal of Global Economic Analysis,* Vol. 1/2, pp. 78–115.

Sadras, V.O., et al. (2017), "Effects of water stress on crop production", *GreenFacts*. www.greenfacts.org/.

Scanlon, B.R. et al. (2007), "Global impacts of conversions from natural to agricultural ecosystems on water resources: Quantity versus quality", *Water Resources Research,* Vol. 45, pp. 1–16.

Schwalm, C.R., S. Glendon and P.B. Duffy (2020), "Rcp8.5 tracks cumulative CO_2 emissions", *Proceedings of the National Academy of Sciences,* Vol. 117/33, pp.19656–19657.

Shamsudduha, M. and R.G. Taylor (2020), "Groundwater storage dynamics in the world's large aquifer systems from grace: uncertainty and role of extreme precipitation", *Earth System Dynamics,* Vol. 11/3, pp. 755–774, https://esd.copernicus.org/articles/11/755/2020/.

Taylor, K.E., R.J. Stouffer and G. Meehl (2012), "An overview of CMIP5 and the experiment design," *Bulletin of the American Meteorological Society,* Vol. 93, pp. 485–498.

WBCSD (2005), *Water Facts and Trends*, World Business Council for Sustainable Development (WBCSD), http://docs.wbcsd.org/.

World Bank (2016), *Climate change action plan 2016–2020*, World Bank Group reports. World Bank, Washington DC.

World Bank (2020), *World Population Prospects 2019*, World Bank Projection, World Bank, Washington DC, https://population.un.org/.

WRI (2022a), *Aqueduct Water Stress Projections*, World Resource Institute, https://resource-watch.org/data/.

WRI (2022b), *Geospatial Datasets*, World Resource Institute, https://datasets.wri.org/dataset/.

Zhao, W. et al. (2020), "Effects of water stress on photosynthesis, yield, and water use efficiency in winter wheat", *Water,* Vol. 12/8, pp. 1–19.

Zolin, C. and R. Rodrigues (eds.) (2020), *Impact of Climate Change on Water Resources in Agriculture*, CRC Press.

Appendix A. Sectors and regions in GTAP-DynW

Table A1. GTAP-DynW Regions

No	Region	Countries included
		North America
1	USA	United States
2	CAN	Canada
3	MEX	Mexico, Rest of North America
		South and Central America
4	BRA	Brazil
5	CAM	Central South America: Costa Rica, Guatemala, Honduras, Nicaragua, Panama, El Salvador, Rest of Central South America, Dominica, Jamaica, Puerto Rico, Trinidad and Tobago
6	NSA	Northern South America: Bolivia, Colombia, Ecuador, Paraguay, Peru, Venezuela, Rest of South America
7	SSA	Southern South America: Argentina, Chile, Uruguay
		Europe and Eurasia
8	CEU	Central Europe: Czech Republic, Estonia, Hungary, Latvia, Lithuania, Poland, Slovakia, Slovenia,
9	DEU	Bulgaria, Croatia, Romania, Germany
10	EEW	East Europe and West Asia: Albania, Belarus, Ukraine, Rest of Eastern Europe, Kazakhstan, Kyrgyztan, Tajikistan, Rest of Former Soviet Union, Armenia, Azerbaijan, Georgia
11	FRA	France
12	GBR	United Kingdom
13	ITA	Italy
14	TUR	Turkey
15	RUS	Russia
16	WEU	Other Western Europe: Austria, Belgium, Denmark, Finland, Greece, Iceland, Ireland, Luxembourg, Netherlands, Norway, Portugal, Spain, Malta, Sweden, Switzerland, Rest of Western Europe
		Middle East
17	ME	Bahrain, Iran, Israel, Jordan, Kuwait, Oman, Qatar, Saudi Arabia, UAE

No	Region	Countries included
Africa		
18	CAF	Central Africa: Benin, Burkina Faso, Cameroon, Cote d'Ivoire, Ghana, Guinea, Nigeria, Senegal, Togo, Rest of Western Africa, Central Africa, South Central Africa, Kenya, Rwanda, Tanzania, Uganda, Rest of Eastern Africa
19	NAF	North Africa: Egypt, Morocco, Tunisia, Rest of North Africa, Ethiopia
20	OSA	Other Africa: Madagascar, Malawi, Mauritius, Mozambique, Zambia, Zimbabwe, Botswana, Namibia,
21	ZAF	Rest of Africa, South Africa
Asia-Pacific		
22	ASEAN	Brunei, Cambodia, Laos, Malaysia, Philippines, Singapore, Thailand, Vietnam, Rest
23	AUS	Australia
24	CHN	China and Hong Kong
25	IND	India
26	JPN	Japan
27	KOR	Korea
28	NZL	New Zealand
29	SAS	South Asia: Bangladesh, Nepal, Pakistan, Sri Lanka, Rest of South Asia
30	EAO	Rest of Oceania, Mongolia, Taiwan, Rest of East Asia

Table A2. GTAP-DynW Sectors

No	Codes	Model Sectors	GTAP V10 Sectors
1	pdr	Paddy rice	Paddy rice
2	wht	Wheat	Wheat
3	gro	Cereal grains nec	Cereal grains nec
4	ocr	Plantation	Vegetables, fruit, nuts; oil seeds; sugar cane, sugar beet; plant-based fibres; crops nec
5	ctl	Livestock	Cattle, sheep, goats, horses
6	oap	Animal products nec	Animal products nec
7	frs	Forestry, fishing	Forestry, fishing
8	coa	Coal	Coal

No	Codes	Model Sectors	GTAP V10 Sectors
9	oil	Oil	Oil
10	gas	Gas	Gas
11	omn	Minerals nec	Minerals nec
12	omt	Livestock Products	Wool, silk-worm cocoons; Meat: cattle, sheep, goats, horse; Meat products nec
13	mil	Dairy	Dairy products, raw milk
14	ofd	Food processing	Processed rice, sugar, food products nec, beverages and tobacco products, vegetable oils and fats
15	tex	Textiles, wear	Textiles; Wearing apparel; Leather products
16	lum	Wood and paper	Wood products, Paper products, publishing
17	p_c	Petroleum, coal products	Petroleum, coal products
18	crp	Chemical, rubber, plastic	Chemical, rubber, plastic prods
19	nmm	Mineral products nec	Mineral products nec
20	i_s	Ferrous metals, Metals nec	Ferrous metals, Metals nec, Metal products Motor vehicles and parts, transport equipment nec
21	omf	Manufacturing	Electronic equipment; Machinery and equipment nec; Manufactures nec
22	ely	Electricity	Electricity
23	gdt	Utilities	Gas manufacture, distribution; Water
24	cns	Construction	Construction
25	otp	Transport nec	Transport nec
26	wtp	Sea transport	Sea transport
27	atp	Air transport	Air transport, Communication; Trade; Financial services
28	obs	Services	nec; Insurance; Business services nec;PubAdmin/Defence/ Health/Educat
29	ros	Recreation	Recreation and other services
30	dwe	Dwellings	Dwellings

Appendix B. Shock variables for climate change scenarios

Table B1. Datasets and shock variables

	Variables	Contents	
		Sets	**Size**
1	i=TRADE−COMM	Traded commodities	30
2	r=REG	Region	30
3	j=FIRM−COMM	Commodities demanded by firms	40
4	b=PROD−COMM	Produced commodities	31
5	c=ENDW−COMM	Endowment commodities	22
6	d=ENDWS−COMM	Sluggish endowments	19
7	e=ENDWL−COMM	Land Endowments (AEZ1-18)	18
8	t=alltime	Time 2022-2100	79
	Selected Intertemporal Shocks for Water Stress's Impacts (%) Average/Region		
		(i) Effect on Land Use with Irrigated Water	
3	dQSEc,t,r	Shock on quantity of AEZ land use in region r (%/year)	-0.1 to -3.1
		(ii) Shock of Water Stress on Agricultural Production (%/year)	
9	dafw1j,t,r	Shock of water stress on agricultural production in region r	0.1 to 5.4

Appendix C. A summary of the WRI methodology for the projection of (blue) water available, water consumption and water stress

Following Luck et al. (2022), the WRI projections were developed primarily by general circulation models from the Coupled Model Inter-comparison Project-Global Circulation Models (CMIP5-GCMs) (Taylor et al., 2012), and SSP scenarios from (IIASA, 2019). The WRI projections provide for 15,006 global basins in the form of GIS spatial layers, including water withdrawal and consumptive use (demand), water supply, water stress and intra- annual (seasonal) variability for the 2020s, 2030s and 2040s by RCP4.5 and RCP8.5-SSP2 and RCP8.5-SSP3.

Water supply and water availability

WRI (2022a) estimates water supply at basin level (for 15,006 basins) from runoff values extracted from an ensemble of CMIP5-GCMs, which provides valuable insights about the climate system and the processes responsible for climate change and variability. More than 20 modelling modules are performing for the 50 CMIP5 model simulations (Taylor et al., 2012). An essential input of CMIP is from the Global Coupled Ocean-Atmosphere General Circulation Models (coupled GCMs), which detect both anthropogenic effects over the past century and project future climate changes due to human activities and energy fuel-mix changes. CMIP has archived output from both constant forcings ("control run") and perturbed (1% per year increasing atmospheric carbon dioxide) simulations using summarised results from 18 CMIP models (Covey et al., 2003). Representing a broad lineage of models from geographically and diverse modelling approaches, six Global Circulation Models (GCMs) were selected to reproduce the mean and standard deviation of historical runoff using macro variables from the RCP4.5 and RCP8.5 scenarios. Several GCMs had results for multiple ensemble members across the two climate scenarios (13 for RCP4.5 and 17 for RCP8.5).In particular, WRI (2022a) fit generalised extreme value (GEV) distributions separately for each pixel over the historical period data (1950–2005) for each GCM run and the corresponding Global Land Data Assimilation System (GLDAS-2) data. The GCM values are corrected by matching distributions.

The WRI water supply indicator is total blue water (renewable surface water), which projected change to be equal to the 21-year mean around the target year divided by the baseline period. Luck et al. (2022) estimate total blue water *Bt* and available blue water (*Ba*) from bias-corrected runoff values, which were resampled to 1 km x 1 km spatial layers and summed into hydrological catchments for the downstream water flow-accumulation in rivers. Following Gassert et al. (2014), WRI (2022*a*) used an approach of sparse catchment- to-catchment flow accumulation to estimate water supply to a catchment.

Water withdrawals and consumption

Water withdrawals and consumption for agriculture, industry and domestic users were projected from historical data and macro-outlooks of GDP, population and urbanisation. The variables employed for water demand projection include area equipped for irrigation; agricul-

tural land area (including both irrigated and rain-fed agriculture); irrigation efficiency; industrial water withdrawals; domestic water withdrawals; GDP per capita; urbanisation; baseline water stress, population density; and world population. While most macro variables are from FAO and World Bank, the baseline water stress for 25,008 global basins are from WRI (2022b) and Gassert et al. (2014). (WRI, 2022a) measures water demand as water withdrawals, with the projected change in water withdrawals equal to the summarised withdrawals for the target year, divided by the baseline year.

Irrigation withdrawals

Agricultural irrigation (by far the most significant withdrawals) is unique among water users because its withdrawals depend strongly on climate (as evaporative demand) and the extent and efficiency of irrigation.

In agriculture, the projected change in water withdrawals (Uag) equals the summarised withdrawals for the target year, divided by the baseline year, 2010. Since water consumptive irrigation use (Cag) varies based on climate, WRI (2022a) estimated Uag and Cag for each year. First, WRI (2022a) projected country-level irrigated area, then spatially distributed the irrigated area within each country and used climate projections to estimate the consumptive use over the projected irrigated area. WRI (2022a) explicitly projected changes in the spatial extent of irrigation to incorporate the effect of climate over-irrigation areas. The projections of the irrigated area by country were estimated using mixed effects regression of space equipped for irrigation ($AEI_{i,t}$) from FAO (2022a) for a country at the year as a function of the socioeconomic variables. To prevent projections from exceeding available agricultural land, the response variable was modelled as the logit-transformed proportion of agricultural land equipped for irrigation in total agricultural land for the country in year t. Luck et al. (2022) employs a fit coefficient to predictor variables, including country-specific intercepts (with specific features of policies, geographical climate conditions, etc. and world population and international agricultural trade). Luck et al. (2022) converted the regression model's projections to the irrigated area by using the predicted proportion (using the inverse-logit function techniques), multiplying by the area irrigated and finally multiplying by the ratio of the area irrigated to the area equipped for irrigation.

The projection of irrigated area at the country level was distributed spatially within countries to pixels based on the likelihood of irrigation expansion (LIE) dataset. For each country and scenario, WRI (2022*i*) projects the change in irrigation area (as the difference between the projected area for the target year and the baseline year).[4] WRI (2022a) generated one estimate of the extent of irrigated area for each of the target decades/years, the 2020s, 2030s and 2040s.

Irrigation consumption

Irrigation consumption was estimated following the FAO methodology of consumptive irrigation use (ICU), excluding crop-specific evapotranspiration factors. ICU is the annual depth

---

[4]WRI (2022a) distributed positive values of the spatial distribution of irrigated area in three steps until all available land in a country was exhausted. First, WRI (2022a) distributed to the area equipped for irrigation but not currently irrigated, starting with the highest likelihood class until available land was located, then proceeding to the next lower likelihood class. Second, WRI (2022a) distributed any remaining areas unequipped for irrigation (but likely to be irrigated in each country), up to a doubling of irrigated area in each class above. Finally, any available space in a country was distributed globally, proportionally to the remaining available area by descending likelihood class, to allow agricultural trade between nations.

of water needed to fulfil the deficit between crop consumption with ample water and crop consumption with rainfed conditions. WRI (2022a) calculated ICU as potential minus actual evapotranspiration.[5]

The irrigation water requirement (IWR) is the water required for optimal crop growth, including consumptive and non-consumptive purposes. The water requirement ratio (WRR), or irrigation efficiency, is the water required by crops to meet their evapotranspiration needs divided by the amount of water withdrawn. This ratio is less than one because of water leakage or other losses in the irrigation system.

Water stress

Following Gassert et al. (2014), the water stress at time t (WS_t) is estimated as the ratio of water withdrawals (UW_t) to available blue water ($Ba5_t$) on an average annual basis.

$$WS_t \equiv \frac{UW_t}{Ba_{[t-10:t+10]}} \tag{13}$$

Available blue water Ba is flow-accumulated run-off minus upstream consumptive use over catchments. WRI (2022a) computed Ba as the mean of the 21 years around the projected year. The baseline is the average value of the 1950–2010 period.

Supplementary information

Model code and supporting data will be made available at https://osf.io/mrbuh/. Please acknowledge any use of these materials and the accompanying manuscript/paper. Users will also require GTAP data.

---

[5]For countries where the irrigated area was projected to decline, WRI (2022a) distributed negative values in reverse order of probability (i.e. removed from least likely to be expanded).

GLOBAL COMMISSION on the ECONOMICS OF WATER

The Global Commission on the Economics of Water (GCEW) redefines the way we value and govern water for the common good.

It presents the evidence and the pathways for changes in policy, business approaches and global collaboration to support climate and water justice, sustainability, and food-energy-water security.

The Commission is convened by the Government of the Netherlands and facilitated by the Organisation for Economic Co-operation and Development (OECD). It was launched in May 2022 with a two-year mandate.

The GCEW is executed by an independent and diverse group of eminent policy makers and researchers in fields that bring novel perspectives to water economics, aligning the planetary economy with sustainable water-resource management.

Its purpose is to make a significant and ambitious contribution to the global effort to spur change in the way societies govern, use and value water.